J. Wind Eng. Ind. Aerodyn. 133 (2014) 1–17

Contents lists available at ScienceDirect

Journal of Wind Engineering and Industrial Aerodynamics

journal homepage: www.elsevier.com/locate/jweia

Large Eddy Simulation of wind farm aerodynamics: A review ☆

D. Mehta [a,b,*], A.H. van Zuijlen [b], B. Koren [c], J.G. Holierhoek [a], H. Bijl [b]

[a] Energy Research Centre of the Netherlands (ECN), Petten 1755 ZG, The Netherlands
[b] Delft University of Technology (TU Delft), Delft 2629 HS, The Netherlands
[c] Eindhoven University of Technology (TU Eindhoven), Eindhoven 5600 MB, The Netherlands

ARTICLE INFO

Article history:
Received 12 March 2014
Received in revised form
16 June 2014
Accepted 9 July 2014

Keywords:
Large Eddy Simulation
Engineering models
Wind farm aerodynamics
Atmospheric boundary layer
Subgrid stress model

ABSTRACT

To study wind farm aerodynamics (WFA), the Wind Power industry currently relies on simple *Engineering Models* (EM) that simulate wind farms using basic principles of physics and empirically established approximations. EMs are fast and accurate for an overview of WFA and gauging mean power production, but cannot resolve phenomena like wake meandering, effect of atmospheric stratification on wake development, a turbine's response to partial wake interaction and yawed inflows etc., and their relation with turbine loading, which require a first principle physics-based model, namely Computational Fluid Dynamics (CFD). Although advances in computer technology have promoted the application of CFD, the study of WFA is yet unworkable with Direct Numerical Simulation, which is the most comprehensive CFD technique. Thus, as a trade-off between cost and detail, researchers must resort to Large Eddy Simulation (LES) to garner thorough knowledge of WFA, which could in succession help the industry improve engineering models. This paper summarises the contributions of various LES investigations into WFA and how they have helped broaden our understanding of the subject. Additionally, the article touches upon the optimal use of LES and of the resultant data, and also the challenges faced by LES.

1. Introduction: Wind Turbine Wakes

Field experiments (Taylor, 1990; Cleijne, 1993; Jensen et al., 2004; Barthelmie et al., 2007), wind tunnel tests (Elliot, 1991; Chamorro and Porté-Agel, 2011) and Computational Fluid Dynamics (CFD) (Barthelmie et al., 2009; Ivanell, 2009) have corroborated that the power delivered by a wind farm is less than the sum of its turbines' rated powers. This stems from the deceleration of the faster freestream atmospheric flow as upstream turbines extract energy from it, producing wakes with reduced velocity (velocity deficit), which later interact with downstream turbines and limit the power they generate. In addition, turbine wakes bear a higher level of turbulence (added turbulence intensity) than that of the freestream flow, which increases the dynamic loading experienced by downstream turbines, in turn reducing their longevity (Thomsen and Sørensen, 1999; Sanderse et al., 2011).

A wind turbine's wake can be divided into two regions, the *near wake* and the *far wake*. The near wake lies immediately behind the turbine and it is characterised by wake expansion that causes the velocity deficit to attain its maximum value between 1D and 2D[1] (Vermeer et al., 2003; Ainslie, 1998). At such proximity, the turbine's design and loading strongly influence wake development. The near wake ends between 2D and 4D when the shear layer created near the blades' tips by the velocity deficit, thickens with downstream distance and merges near the wake's centre line (Ainslie, 1998; Crespo et al., 1999a). Numerical methods that resolve the near wake must model the rotor accurately and capture the trailing vorticity, the *tip vortices* in particular, which mix the slower wake with the faster freestream. To ensure that the tip vortices are not spuriously transported (in terms of vortex lifetime), near wake methods should also model the *atmospheric boundary layer* (ABL) correctly. The instability incurred by the shear layer due to the breakdown of tip vortices, generates enough turbulence to transition into the far wake (Sørensen, 2011). This is why the added turbulence intensity is noticed to attain a peak

☆This document is a collaborative effort.

* Corresponding author at: Energy Research Centre of the Netherlands (ECN), Petten 1755 ZG, The Netherlands.
E-mail address: mehta@ecn.nl (D. Mehta).

[1] Distances to points downstream of a turbine would henceforth be mentioned as *nD*, where *n* is a positive integer and *D* is the turbine's rotor's diameter

http://dx.doi.org/10.1016/j.jweia.2014.07.002
0167-6105/

value in the transition zone between 3D and 6D (Smith and Taylor, 1991; Wu and Porté-Agel, 2012; Chamorro and Porté-Agel, 2009).

In the far wake, the flow is influenced indirectly by the turbine in terms of the velocity deficit and enhanced turbulence that it creates (van der Pijl, 2007). There are three main sources of turbulence: atmospheric (surface roughness and heating), mechanical (rotor and tower) and the shear layer due to the breakdown of tip vortices. Turbulence from these sources promotes turbulent mixing in the wake that reduces the velocity deficit and turbulence intensity (Sanderse et al., 2011). The velocity deficit is generally negligible beyond 10D (Ammara et al., 2002) but the increased turbulence intensity is sensible as far as 15D (Taylor, 1990). To model the far wake, early numerical methods assumed that the vertical profiles of velocity deficit and turbulence intensity are roughly *Gaussian*, self-similar and even axisymmetric in the far wake, for the sake of simplicity. In addition, the turbulence was treated as isotropic and homogeneous (Crespo et al., 1999a, 1985; Ainslie, 1985). Other approximations for modelling the turbines and ABL enabled the use of these methods for wind farm simulations. However, the use of simplified models was discontinued following evidence that did not support their approximations (Elliot, 1991; Schelz et al., 2001; Gómez-Elvira et al., 2005). Nonetheless, the early models influenced the development of the more advanced *far-wake engineering models*, which are now widely employed by the industry being affordable, speedy and quite accurate in terms of predicting the mean power generation. A brief account of simple velocity-deficit formulations is provided in Section 2.2.

Unfortunately, the performance of engineering models relies heavily on pre-tuning with field data. For example, most engineering models resolve the wake turbulence with *Reynolds-Averaged Navier–Stokes* (RANS) models, the model constants of which must be predetermined using aerodynamic data from wind farms. However, the scarcity of field data prevents comprehensive tuning and renders engineering models suitable only for industrial applications and not for gaining insight into the fundamental physics of wind farm aerodynamics, which demands first principle physics-based models like Large Eddy Simulation (LES) and Direct Numerical Simulation (DNS). Current computational resources only permit the use of LES for high-Reynolds number flows like wind turbine wakes.

Over the last decade, LES has facilitated the study of wind farm aerodynamics and enabled the analysis of phenomena like gusts, atmospheric stratification and even the effect of wind farms on local weather. The aim of this paper is to summarise these contributions of LES and explain how LES could be further developed to improve engineering models, which would remain the industrial workhorse until computational resources enable their replacement with LES.

Section 2 provides a brief summary of the Navier–Stokes (NS) equations, RANS, early wake models and engineering models. For more details, the readers may refer to reviews by Vermeer et al. (2003), Crespo et al. (1999a), Snel (2003, 1998), Hansen et al. (2006) and the more recent one by Sanderse et al. (2011). For succinctness, this paper does not summarise LES studies on rotor, near wake or single turbine aerodynamics, details on which can be found in the above reviews.

Sections 3 and 4 provide a description of LES and summarise various LES studies of wind farm aerodynamics, respectively, followed by a summary of the article in Section 7 and a brief discussion. For information beyond the scope of this paper, the readers are referred to the following books: on wind energy (Hansen, 2008; Burton et al., 2001), on meteorology (Panofsky and Dutton, 1984; Stull, 1998), on LES (Sagaut, 2006; Geurts, 2004), on turbulence (Davidson, 2004; Tennekes and Lumley, 1972) (for a mathematical approach to turbulence Foias et al., 2001) and on CFD (Wilcox, 2006; Perić and Ferziger, 2002; Wesseling, 2001).

2. A brief history of wind farm wake aerodynamics

To appreciate the importance of LES, one must understand the benefits and limits of simpler far wake models that have been used to study wind farm aerodynamics or at least wake interactions of multiple turbines in the ABL. These models are outlined in this section along with a concise description of the NS equations and RANS modelling.

2.1. The Navier–Stokes equations and the statistical nature of turbulence

It is widely accepted that the incompressible form of the NS equations can model the flow around a wind turbine and in its wake, provided that the wind turbine has been accurately parametrised as an external force in the NS equations (Vermeer et al., 2003). Whilst the tip speed of large turbines might approach the limit of incompressibility (~Mach 0.3 at sea level), the flow in the wake remains incompressible (van der Pijl, 2007).

Before beginning with the equations, the authors would like to mention that common variables and symbols are used throughout this paper, as explained in Davidson (2004), Tennekes and Lumley (1972), Perić and Ferziger (2002) and Porté-Agel et al. (2011). The NS equations in Einstein's indicial notation read (the subscript o denotes the reference density and temperature),

$$\frac{\partial u_i}{\partial x_i} = 0, \tag{1}$$

$$\frac{\partial(\rho_o u_i)}{\partial t} + \frac{\partial(\rho_o u_i u_j)}{\partial x_j} = -\frac{\partial p}{\partial x_i} + \frac{\partial}{\partial x_j}\left(\mu\left(\frac{\partial u_i}{\partial x_j} + \frac{\partial u_j}{\partial x_i}\right)\right) + \rho_o f_i + \rho_o g\frac{(\theta - \langle\theta\rangle)}{\theta_0} + f_c \varepsilon_{ij3} u_j, \tag{2}$$

where p is the pressure, μ the molecular viscosity, u_i the component of velocity along the ith direction, t the time and x_i the position vector. Further, $f_c \varepsilon_{ij3} u_j$ is the *Coriolis force*[2] that is pertinent only while analysing wind farms that are spread over a large area (Porté-Agel et al., 2010). The term $\rho_o g(\theta - \langle\theta\rangle)/\theta_o$, g being the acceleration due to gravity, is *Boussinesq's approximation* of the buoyant force on a volume of fluid arising from minor variations in density brought about by changes in temperature (Boussinesq, 1877). The angled brackets stand for an averaged value, for example, over horizontal planes parallel to the ground in a case of an ABL simulation. Thermally generated turbulence in a *non-neutral* ABL can be resolved using an additional scalar transport equation with the *potential temperature* (θ) as the transported variable,

$$\frac{\partial \theta}{\partial t} + \frac{\partial(\theta u_j)}{\partial x_j} - \alpha\frac{\partial^2 \theta}{\partial x_j^2} = q_v, \tag{3}$$

where α is the thermal diffusivity of the medium (air in this case) and q_v is a source of heat or a sink. The above equation need not be solved for a neutral ABL that does not bear any thermally generated turbulence. In this case, $\rho_o g(\theta - \langle\theta\rangle)/\theta_o$ is also ignored in Eq. (2). For an incompressible flow, $\partial u_i/\partial x_i = 0$ and in the absence of heat sources or sinks, the above equation simplifies to,

$$\frac{\partial \theta}{\partial t} + u_j\frac{\partial \theta}{\partial x_j} - \alpha\frac{\partial^2 \theta}{\partial x_j^2} = 0. \tag{4}$$

Turbulence is characterised by regions of swirling fluid known as *eddies* that vary in length throughout the flow. Resolving turbulence with the above equations is challenged by the non-linearity of the convective term, $\rho_o u_i u_j$, which continually gives rise to

[2] δ_{ij} is *Kronecker's delta* and ε_{ijk} is the *Levi–Civita* symbol for three dimensions.

smaller eddies through *vortex stretching* (Perić and Ferziger, 2002). As the Reynolds number of a flow increases, the smaller eddies further reduce in size, creating a greater range of eddy length scales and precluding an exact numerical analysis of such flows with the above equations (Davidson, 2004). So, the dominant approach for investigating turbulence involves the statistical analysis of the flow in the form of averages, as a trade-off between insight and computational requirements (and the resolution of experimental apparatus). The *averaging* leads to the removal of certain length (and time) scales, rendering the system more *solvable*. But such an approach is hindered by the *closure problem* of turbulence, in which, the unknowns that represent the flow's variables, exceed the equations in number (Perić and Ferziger, 2002). To bypass this, scientists resort to mathematical models that relate the unknowns to the physical nature of the flow as consistently as possible (Tennekes and Lumley, 1972). Such mathematical models form the basis of two famous statistical approaches: RANS and LES.

RANS involves decomposing a turbulent variable into the sum of an average and a fluctuating quantity as,

$$\mathbf{u} = \overline{\mathbf{u}} + \mathbf{u}', \tag{5}$$

where $\mathbf{u}$ is a vector and $\overline{\mathbf{u}}$ is its *ensemble average* over many realisations of the flow. Upon decomposing the variables in the NS equations (and dividing throughout by the density) one obtains the RANS Eqs. (6) and (7), which are then solved to obtain $\overline{\mathbf{u}}$.

$$\frac{\partial \overline{u}_i}{\partial x_i} = 0, \tag{6}$$

$$\frac{\partial(\rho_o \overline{u}_i)}{\partial t} + \frac{\partial(\rho_o \overline{u}_i \overline{u}_j)}{\partial x_j} = -\frac{\partial \overline{p}}{\partial x_i} + \frac{\partial}{\partial x_j}\left(\mu\left(\frac{\partial \overline{u}_i}{\partial x_j} + \frac{\partial \overline{u}_j}{\partial x_i}\right)\right) - \frac{\partial \tau_{ij}^{\mathcal{R}}}{\partial x_j} + \rho_o \overline{f}_i + f_c \varepsilon_{ij3} \overline{u}_j + \rho_o g \frac{(\overline{\theta} - \langle \overline{\theta} \rangle)}{\theta_0}, \tag{7}$$

where, the term $\tau_{ij}^{\mathcal{R}}$, that is in fact equal to $\overline{u_i' u_j'}$, arises from the decomposition of the convective term and dictates the transport of mass and momentum due to the fluctuating quantity $\mathbf{u}'$. $\tau_{ij}^{\mathcal{R}}$ represents the *closure problem* and must be modelled in terms of known ensemble-averaged flow variables.

Boussinesq's hypothesis (different from *Boussinesq's approximation*, which was mentioned earlier) is a common approach for modelling $\tau_{ij}^{\mathcal{R}}$ but demands the specification of certain model constants, which are determined empirically and in most cases by assuming that the turbulence is *isotropic* (Sanderse et al., 2011 provide a detailed discussion). Thus, with the exception of the *Reynolds Stress model*, most RANS models are not suitable for the analysis of anisotropic flows, which in the context of wind farm aerodynamics, alludes to the ABL and turbine wakes (see Section 5).

Additionally, RANS models are often stabilised with artificial (or numerical) diffusion that is generally introduced with *upwind schemes*. This spurious dissipation causes the wakes to recover faster than they should, which must then be curbed by appropriate specification of model constants (Cabezón et al., 2011). Nonetheless, RANS equations have formed the backbone of various engineering models because they provide a speedy and reasonably accurate solution upon correct specification of their model constants.

2.2. Far wake modelling

Although the following description of traditional far wake models is short, it should suffice as a starting point for this paper and shed light on far wake models, their current status and limitations. Detailed information can be found in the reviews (Crespo et al., 1999a; Vermeer et al., 2003).

As an adjunct, it would be wise to briefly describe common formulations for the decay of velocity deficit and turbulence intensity. Crespo and Hernández (1993, 1996) noticed that the decay in velocity deficit and turbulence intensity, is proportional to the downstream distance raised to negative exponents of nearly $-2/3$ and $-1/3$, respectively, leading to a simple power law. Regression fits between velocity deficit and downstream distance from SODAR (Sonic Detection and Ranging) measurements at the Vindeby offshore farm in Denmark, led to an exponent of nearly 1 (Barthelmie et al., 2004), suggesting that the exponents depend on the ambient turbulence, the inflow profile, ABL stratification etc.

Recently, based on the principles of mass and momentum conservation and assuming a *Gaussian* profile for the velocity deficit, Bastankhah and Porté-Agel (2014) proposed an *exponential model* of velocity distribution in the wake. The formulation also accounts for the asymmetry due to the shear in the ABL and variations in velocity along the spanwise direction. Comparison with LES studies and high-resolution wind tunnel data revealed that the formulation was accurate as compared to a simpler model like the wake-effect model in WAsP (Wind Atlas Analysis and Application Program) (Jensen, 1983), which assumes that the wake expands linearly in diameter with downstream distances. The rate of expansion is determined by the turbulence intensity. Another model based on wake expansion is that of Frandsen et al. (2006), which is adapted to regimes that include infinite wind farms, multiple-wake flow and changes in surface roughness, while considering the presence of the ground that causes asymmetric wake expansion.

2.2.1. Individual wakes

Individual wakes were first analysed with quick *Kinematic models* as self-similar profiles of velocity deduced from studies on jets (Lissaman, 1979; Abramovich, 1963). The input profile at the end of the wake's expansion region could be modulated to specify the correct velocity deficit using the turbine's thrust coefficient. Despite various attempts to make Kinematic models comprehensive, their dependence on the proper specifications of model parameters, inability to model wake meandering and the hypothesis of self-similarity that is violated by the presence of the ground, remained major drawbacks.

On the other hand, *Field models* solved the parabolic NS equations by ignoring the turbulent diffusion and the gradient of pressure along the main flow direction (Sforza et al., 1981; Ainslie, 1985). This not only helped simplify the model, but also reduced the computational time significantly (Cabezón et al., 2011). Field models were validated successfully against wind tunnel tests and could also account for large scale effects like wake meandering, albeit with necessary modifications. However, the assumption of an axisymmetric wake, prevented the deviation of velocity and turbulence profiles from axisymmetry and hence enforced two-dimensionality, as reported by experiments.

Boundary Layer wake models were a major improvement over their predecessors in terms of treating the wake as non-axisymmetric and introducing three-dimensionality, along with more detailed modelling of the ABL using Monin–Obukov's approach (Moeng, 1984). The meandering of the wake could also be predicted with a simple modification. The turbulent wake was *modelled* with the $\kappa - \epsilon$ RANS model, although in a parabolic sense. An elliptic formulation, which incorporated the gradient of pressure and turbulent diffusion along the main flow direction (in essence, the RANS equations), was also proposed (Cabezón et al., 2011). However, the improvements were disproportionate with the increased computational needs. Despite treating the turbulence as anisotropic, the overall performance was still dependent

on the accurate specification of RANS model parameters and the initial wake deficit.

2.2.2. Multiple wakes and wind farms

The *Surface Roughness* models were amongst the first and simpler wind farm models. They used a logarithmic profile for the ABL and modelled the turbines as elements of extra roughness. Frandsen used two profiles, one for the flow between the ground and the turbines' hubs and another above the turbines' hubs to model the turbines' action as a drag force (Frandsen, 1992). Despite its simplicity, Frandsen's model proved useful in the study of the effect of large offshore wind farms on local weather (Crespo et al., 1999b) and was also improved later with the application of LES (see Section 4.3).

A proper treatment of wakes was first done with *Superposition* models, in which the velocity perturbations caused by multiple turbines were superimposed to model their combined effect. Semi-empirical modifications were made to account for the fact that downstream wakes recover more rapidly due to enhanced turbulence intensity. This was replicated correctly in the data that Superposition models produced on power generation, which dropped significantly for the first two rows of turbines with no measurable decrease for more downstream rows. The downside of these models was the lack of physical justification for the algorithms used for superimposing the wakes.

Wind farm codes witnessed a major improvement with the advent of parabolic formulations of single wake models. Initially, all turbines were modelled as profiles of velocity deficit and added turbulence intensity allocated at the end of the wake's expansion region, which would then be transported downstream. This was later replaced with the method of assigning perturbations of flow variables at the turbine's location, and finally by actuator methods (ref. Sanderse et al., 2011).

Although elliptic formulations of wind farm wake models were also proposed, their the improvements were not in proportion to the increased computational requirements. Further, elliptic models resolve the turbulence accurately in the far wake, but tend to be too diffusive in the near wake and under predict the velocity deficit unless the model's coefficients in the RANS equations are tuned appropriately. By neglecting streamwise diffusion, parabolic models predict the velocity deficit correctly in the near wake but underestimate it in the far wake, while overestimating the turbulence intensity. Amongst RANS models, the Reynolds Stress model that does not rely on Boussinesq's hypothesis and permits the anisotropic resolution of the fluid, provides the most reliable results in both the near and the far wake. However, in the near wake it still under predicts the velocity deficit by a small amount, which could be tackled by careful tuning.

In short, elliptic models are suitable for far wake analyses that are relevant to wind farms as they predict both the turbulence intensity and velocity deficit correctly in the far wake, which comprise the inflow for the downstream turbines. Results can generally be improved with advanced RANS models, like the Reynolds Stress model, or with more careful specification of model parameters. On the other hand, parabolic models are good only for the near wake. A detailed comparison of elliptic and parabolic models can be found in Cabezón et al. (2011).

2.2.3. Summary

To summarise, far wake models must be able to correctly predict the turbulence intensity and velocity deficit at distances greater than 7-8D, a normal separation for turbines on a modern wind farm. The use of RANS models instead of LES, is wise to save computational effort but increases the dependency on tuning. Most engineering models perform inaccurately for a single inflow direction, however their predictions are reasonably accurate when averaged over a range of inflow angles (Barthelmie et al., 2009). The inability to generate proper results for a single inflow direction stems from the combination of inaccurate turbulence and ABL modelling, tuning with limited field data and the inability to resolve the flow in case of multiple turbine-wake or wake-wake interactions. It is fair to mention that good turbine modelling is important for the proper function of *engineering models* and the simple allocation of velocity profile at the end of the near wake is certainly not the most accurate initial condition.

Details on the validity of *Boussinesq's hypothesis*, RANS modelling and its application to wind turbine aerodynamics can be found in (Davidson, 2004; Wilcox, 2006; Schmitt, 2007; Réthoré, 2009; Sanderse et al., 2011).

3. Large eddy simulation

From the last section, one may conclude that engineering models (using RANS) are suitable for industrial use, especially when statistics on mean flow and power are desired. But to comprehend the physics of wind farm aerodynamics, one requires a more sophisticated technique that *resolves* most eddies of the flow, at least those which are relevant to wake evolution and power production, instead of modelling them. This is not only of academic interest, but also bears relevance to the industry, which requires detailed knowledge on the performance of wind turbines post-deployment, off-design performance, for example in the presence of gusts, atmospheric stratification etc.

DNS is a comprehensive technique that resolves all the eddies of a flow. However, the flow through a wind farm comprises eddies that range in size from the blade's boundary layer to the distance between successive turbines, due to the flow's high Reynolds number ($\sim 10^7$, based on freestream velocity and turbine diameter). This unfortunately makes DNS unworkable with today's computational means.

As an alternative, a technique like LES that permits the mathematical modelling of certain eddies, to remove information from the flow (or reduce the degrees of freedom) and resolve the rest with the *filtered NS* equations, could be more practicable. The eddies that actually resolved should be the ones that are most relevant to understanding wind farm aerodynamics. On a wind farm, these eddies would be the turbulent structures that are comparable with or larger than the turbine's diameter and are responsible for the transport of mass, momentum and energy.

This section provides a concise description of LES and the mathematical models it employs.

3.1. Eddies and the energy spectrum

Leonard (1974) defines LES as “using a more tractable form of the NS equations, to *approximate while retaining*, the most energetic features of the undisturbed problem”. The eddies of a turbulent flow can be divided into three regimes:

- The large energy-containing eddies that are unaffected by molecular viscosity and carry most of the flow's energy.
- The intermediate inertial scales that are unaffected by viscosity, boundary conditions and the large scales.
- The small *Kolmogorov* (or dissipative/small) scales that are strongly affected by molecular viscosity.

LES *resolves* all scales except for those comparable in size to the *Kolmogorov* scales (and the smaller scales of the inertial range, to be more precise) at which dissipation is dominant. The smallest scales that could be resolved with LES or should be resolved for an

accurate LES, depend on the flow's Reynolds number that determines how wide is the range of length scales, the computational resources that set the limit on resolution and the type of data that is desired from an LES, mean flow quantities or detailed local information about the flow (ref. Liu et al., 1994 for such an analysis). Instead of being resolved, these small scales are modelled with a *Subgrid Scale* (SGS) model. Initially, LES was built upon two assumptions (Frisch, 1995):

- The Kolmogorov scale is universally invariant regardless of the flow's nature, i.e. small scale turbulent motions are statistically identical for high Reynolds number turbulent fields. Further, at this scale the flow loses its directionality and becomes statistically isotropic (Pope, 2000).
- *Scale Invariance* is an integral property of the *inertial range*, i.e. turbulent motions occur simultaneously at different scales at nearly the same location (Meneveau and Katz, 2000) (also Lesieur and Metais, 1996).

Kolmogorov expressed the second point in a mathematical sense by studying the relation between the energy content of an eddy and its size, now known as the *energy spectrum*. A dimensional analysis hinted at the scale invariance of the rate of dissipation of large scale Turbulent Kinetic Energy (TKE) due to molecular viscosity or ε as,

$$E(k) = c_K \epsilon^{2/3} k^{-5/3}, \tag{8}$$

where c_K is the Kolmogorov constant and k is the wave number, which is related to the eddy's size (Meneveau and Katz, 2000). The quantity $\gamma^{5/3}E(\gamma k)$ is invariant in the inertial range under scale transformation i.e. $k \rightarrow \gamma k$ (γ is a real number). It is this symmetry that helps link the dynamics of the large and small scales in the modelling of turbulence.

The assumptions of *scale invariance* have been confirmed experimentally and numerically for but a handful of situations. These might not always hold true, especially outside of the inertial range (Meneveau and Katz, 2000). Thus, SGS models to replace smaller scales for LES are a theoretical (or experimental) approximation and their utility is much dependent of the flow's nature and the desired turbulence statistics, as it would be seen later.

3.2. Filtered Navier–Stokes equations

Based on modelling the interaction of the dissipative scales with the resolved large scales, LES may be classified as being *Implicit* or *Explicit*.

Implicit LES treats the action of the subgrid scales on the resolved scales as purely dissipative. One employs an upwind scheme to discretise the convective term or uses an artificial dissipative term to introduce dissipation, which in general, is very close to that introduced by a physical model (explicit LES). In practice, the numerical dissipation is second or fourth-order accurate. Various methods of Implicit LES are mentioned in Sagaut (2006), for a detailed description the readers are referred to Grindstein et al. (2007).

Explicit LES that has been the popular approach, uses an SGS model to represent the coupling between the resolved and the subgrid scales. One of simplest explicit LES models, the Smagorinsky model, formulates the coupling based on the equilibrium between the flow of kinetic energy from the resolved scales and its dissipation by the subgrid scales. This approach is known as *functional modelling*. On the other hand is *structural modelling*, which seeks to reproduce the statistical correlations between the large-scale structures at different scales (Sagaut, 2006). Bardinas Scale-Similarity model falls under this category (Bardina et al., 1983). A detailed explanation of the assumptions, principles and limitations of Implicit and Explicit LES is beyond the scope of this paper. However, the explicit models that have been used for the simulation of wind farm aerodynamics, have been explained briefly in Section 3.3.

In LES, the smallest eddy that can be represented on the grid, is a function of the grid's resolution. Thus, the NS equations must be modified to govern the dynamics of only the resolved scales in an LES. This modification is best explained in terms of a *filter*.

A filter is an operator that is *high-pass* in scale size and removes eddies that are smaller than the filter's *cut-off width* (or length). The cut-off width must be large in comparison to the Kolmogorov scale, ideally somewhere in the inertial range. Filtering a turbulent vector variable $\boldsymbol{x}$, with a filtering operator $\mathcal{G}$, decomposes $\boldsymbol{x}$ into a filtered and a residual quantity,

$$\mathcal{G} * \boldsymbol{x} = \widetilde{\boldsymbol{x}} + \boldsymbol{x}', \tag{9}$$

where $\widetilde{\boldsymbol{x}}$ is the filtered (or resolved) component that represents the large scales. In practice, the cut-off width (denoted later by Δ) is equal to the grid-size (denoted later by h_g). So, the residual component represents the eddies that are smaller than the grid-size, which are hence identified in LES as the *subgrid scales*. RANS is based on a similar approach where $\mathcal{G}$ is an ensemble average, as mentioned earlier.

Filters for LES are based on convolution as proposed by Leonard (1974) and described as,

$$\mathcal{G} * \boldsymbol{\phi}(\boldsymbol{x}) = \int \boldsymbol{\phi}(\boldsymbol{\xi}) G(\boldsymbol{x} - \boldsymbol{\xi}) d^3\boldsymbol{\xi}, \tag{10}$$

where the convolution kernel G is a function of the cut-off scale in space and obeys (Germano, 1987):

$$\int G(\boldsymbol{x} - \boldsymbol{\xi}) d^3\boldsymbol{\xi} = 1, \tag{11}$$

$$\widetilde{\boldsymbol{\phi}} + \widetilde{\boldsymbol{\psi}} = \widetilde{\boldsymbol{\phi} + \boldsymbol{\psi}} \quad \text{and} \tag{12}$$

$$\frac{\widetilde{\partial \boldsymbol{\phi}}}{\partial n} = \frac{\partial \widetilde{\boldsymbol{\phi}}}{\partial n}. \tag{13}$$

$\mathcal{G}$ is generally *Top Hat/Box*, *Gaussian* or *Spectral/Sharp Cut-Off* for a spatial filter (details in Pope, 2000). Upon filtering the incompressible NS equations in the absence of body forces one obtains,

$$\frac{\partial \widetilde{u}_i}{\partial x_i} = 0, \tag{14}$$

$$\frac{\partial(\rho_o \widetilde{u}_i)}{\partial t} + \frac{\partial(\rho_o \widetilde{u_i u_j})}{\partial x_j} = -\frac{\partial \widetilde{p}}{\partial x_i} + \frac{\partial}{\partial x_j}\left(\mu\left(\frac{\partial \widetilde{u}_i}{\partial x_j} + \frac{\partial \widetilde{u}_j}{\partial x_i}\right)\right) + \rho_o f_i + \rho_o g \frac{(\widetilde{\theta} - \langle \widetilde{\theta} \rangle)}{\theta_0} + f_c \varepsilon_{ij3} \widetilde{u}_j. \tag{15}$$

It is important to mention that there is *no explicit filtering* involved in LES. The *tilde* only implies that the above equations pertain to the resolved scales alone. Thus, one begins with a velocity field that contains only those fluctuations that can be assigned to the LES grid (or the filtered components). All velocity fluctuations below the grid's size[3] (or the residual/subgrid scale components) are not present in the field, which is hence the filtered field. But explicit filtering is used in conjunction with some SGS models, which will be described later.

Decomposing the filtered convective term $\widetilde{u_i u_j}$ is not straightforward and incurs the *closure problem* for Explicit LES. Leonard addressed this issue by decomposing the term as,

$$\tau_{ij} = \widetilde{u_i u_j} - \widetilde{u}_i \widetilde{u}_j, \tag{16}$$

[3] $h_g = \sqrt[3]{\prod_{i=1}^{3} h_i}$ for 3-D, where h_i is the average grid size along the ith direction.

where τ_{ij} is the subgrid stress tensor, which is modelled with an SGS model. Thus, the momentum equation for the LES of an incompressible flow reads,

$$\frac{\partial(\rho_o\widetilde{u}_i)}{\partial t}+\frac{\partial(\rho_o\widetilde{u}_i\widetilde{u}_j)}{\partial x_j}=-\frac{\partial\widetilde{p}}{\partial x_i}+\frac{\partial}{\partial x_j}\left(\mu\left(\frac{\partial\widetilde{u}_i}{\partial x_j}+\frac{\partial\widetilde{u}_j}{\partial x_i}\right)\right)-\frac{\partial\tau_{ij}}{\partial x_j}+\rho_o f_i+\rho_o g\frac{(\widetilde{\theta}-\langle\widetilde{\theta}\rangle)}{\theta_0}+f_c\varepsilon_{ij3}\widetilde{u}_j. \quad (17)$$

Similarly, the filtered equivalent of Eq. (4) reads,

$$\frac{\partial\widetilde{\theta}}{\partial t}+\widetilde{u}_j\frac{\partial\widetilde{\theta}}{\partial x_j}-\alpha\frac{\partial^2\widetilde{\theta}}{\partial x_j^2}=-\frac{\partial q_j}{\partial x_j}, \quad (18)$$

where q_j is the SGS flux of heat and $\widetilde{\theta}$ is the filtered potential temperature. Akin to τ_{ij}, q_j in the above equations is expressed as,

$$q_j=\widetilde{u_j\theta}-\widetilde{u}_j\widetilde{\theta}. \quad (19)$$

For details on the parametrisation of the SGS heat flux with an *eddy-diffusivity model*, the readers are referred to Porté-Agel (2004), Porté-Agel et al. (2011). The authors would like mention again that the transport equation for the potential temperature need only be solved for a non-neutral ABL, examples of which can be found in Porté-Agel et al. (2014).

3.3. Subgrid scale models

Most wind farm LES codes use *eddy-viscosity models* to model the subgrid scales. These models relate the SGS dissipation with the resolved velocity field, through a local value of *eddy viscosity*. This section describes three eddy-viscosity models in increasing order of complexity.

3.3.1. Smagorinsky's model (SM)

Smagorinsky (1963) parametrised the SGS stresses by expressing their *deviatoric components* as,

$$\tau_{ij}-\frac{1}{3}\delta_{ij}\tau_{kk}=-2\nu_T\widetilde{S}_{ij}, \quad (20)$$

where ν_T is the eddy viscosity and $\widetilde{S}_{ij}$ is the *resolved strain rate tensor*, which are expressed in terms of the resolved velocity field as,

$$\nu_T=(C_S\widetilde{\Delta})^2|\widetilde{S}_{ij}|, \quad (21)$$

$$\widetilde{S}_{ij}=\frac{1}{2}\left(\frac{\partial\widetilde{u}_i}{\partial x_j}+\frac{\partial\widetilde{u}_j}{\partial x_i}\right) \quad \textit{and} \quad (22)$$

$$|\widetilde{S}_{ij}|=(2\widetilde{S}_{ij}:\widetilde{S}_{ij})^{1/2}. \quad (23)$$

$\widetilde{S}_{ij}:\widetilde{S}_{ij}$ is the magnitude of the tensor $\widetilde{S}_{ij}$. The *tilde* over Δ represents the spatial cut-off scale associated with the filtering operator $\mathcal{G}*x=\widetilde{x}+x'$. In practice, one could set $\widetilde{\delta}$ equal to the overall grid-size i.e. h_g. However, one is free to choose a value greater than h_g, in which case, the above equations only model all scales smaller than $\widetilde{\delta}$.

Lilly (1967) estimated that $C_S\sim0.17$ for isotropic homogeneous turbulence. As expected, using Lilly's value of C_S for an inhomogeneous and anisotropic flow, such as a wall-bounded flow would lead to spurious results with Smagorinsky's model (Bou-Zeid et al., 2005; Porté-Agel et al., 2000). This was first corrected by Mason (1989) with a *ad hoc* damping function to dampen the SGS mixing length near walls to alter the value of C_S, which has been used in wind farm LES codes.

Smagorinsky's model is purely dissipative by construction and does not permit the backscatter of energy from the dissipative scales to the resolved scales, as confirmed experimentally (Liu et al., 1994). This dissipative nature causes the mean shear and streamwise velocity near a wall to be over predicted, leading to a faulty velocity profile (Porté-Agel et al., 2000). The absence of such dissipation is essential while simulating the ABL to avoid dampening its large scales that interact with the wake to transport momentum and energy (see Section 4.3).

3.3.2. Standard dynamic model

A drawback of Smagorinsky's model is that it uses a constant value of C_S that was noticed to decrease with an increase in mean shear and anisotropy (Horiuti, 1993). Being dissipative by construction, using a high value of C_S such as 0.17 leads to excessive subgrid dissipation of TKE and the premature decay of large scale turbulence.

Germano (1992) proposed the Standard Dynamic model (SDM) based on what is now known as the *Germano identity*, which uses a second filter[4] called the *test filter* to relate the turbulent stresses at different scales to obtain a locally isotropic value of C_S for inhomogeneous turbulence (Germano et al., 1991; Sagaut, 2006). The test filter's cut-off width $\overline{\Delta}$ is generally set to $2\widetilde{\Delta}$, or twice size of the grid's cells. The subgrid tensor at the test filter's scale $\mathcal{T}_{ij}$, is related to that at the simulation filter's scale or τ_{ij} through,

$$\mathcal{T}_{ij}=\underbrace{\overline{\widetilde{u}_i\widetilde{u}_j}-\overline{\widetilde{u}_i}\,\overline{\widetilde{u}_j}}_{\mathcal{L}_{ij}}+\overline{\tau}_{ij}, \quad (24)$$

where $\mathcal{L}_{ij}$ is the *resolved stress tensor* arising from *Germano's decomposition* and can be evaluated using the filtered velocity field. Smagorinsky's model helps relate $\mathcal{L}_{ij}$ to the *strain rate tensor at the simulation scale filtered at the test filter's scale*,

$$\mathcal{T}_{ij}-\frac{1}{3}\delta_{ij}\mathcal{T}_{kk}=-2(C_{S,\overline{\Delta}}\overline{\Delta})^2|\overline{\widetilde{S}}|\overline{\widetilde{S}}_{ij}, \quad (25)$$

where $C_{S,\overline{\Delta}}$ is the value of C_S at scale $\overline{\Delta}$. For $\overline{\Delta}=2\widetilde{\Delta}$, obtaining $\overline{\tau}_{ij}$ from Smagorinsky's identity and substituting it along with Eq. (25) in Eq. (24) leads to,

$$\mathcal{L}_{ij}-\frac{1}{3}\delta_{ij}\mathcal{L}_{kk}=C_S^2\mathcal{M}_{ij}, \quad (26)$$

where $\mathcal{M}_{ij}$ equals,

$$\mathcal{M}_{ij}=2\widetilde{\Delta}^2(\overline{|\widetilde{S}|\widetilde{S}_{ij}}-4|\overline{\widetilde{S}}|\overline{\widetilde{S}}_{ij}), \quad (27)$$

The above is possible only if it is assumed that C_S is *scale invariant* or

$$C_{S,\overline{\Delta}}=C_{S,\widetilde{\Delta}}=C_S. \quad (28)$$

Lilly (1992) used the method of *least squares* to solve this over-determined system (6 equations, 1 unknown i.e. C_S) by minimising the error,

$$e_{ij}=\mathcal{L}_{ij}-\frac{1}{3}\delta_{ij}\mathcal{L}_{kk}-C_S^2\mathcal{M}_{ij}, \quad (29)$$

from which C_S is obtained as,

$$C_S^2=\frac{\mathcal{L}_{ij}\mathcal{M}_{ij}}{\mathcal{M}_{ij}\mathcal{M}_{ij}}. \quad (30)$$

Apart from the scale-invariance of C_S, the SDM assumes that C_S does not show significant spatial variation below the test filter's scale. This incurs some numerical instability while using the *least squares* approach, which must be eliminated through suitable averaging (Ghosal, 1999).

Averaging may be done over planes (like those parallel to the wall for wall-bounded flows) or a direction in which the flow is statistically homogeneous, known as *planar* averaging (Germano, 1986; Porté-Agel et al., 2000; Lilly, 1992). But with the presence of wind turbines, the flow is no longer homogeneous along the

[4] In LES, this is the *first* clear-cut filter because the grid itself is the primary filter and represents the filtered/resolved velocity field (see Section 3.2).

planes parallel to the ground. Thus, alternative strategies like *local* averaging over neighbouring points (Zang et al., 1993; Basu and Porté-Agel, 2006) and *Lagrangian* averaging over pathlines (Bou-Zeid et al., 2005; Stoll and Porté-Agel, 2006) are more appropriate.

As an improvement over Smagorinsky's model, the SDM could account for backscatter, making it relatively less dissipative (Mason and Brown, 1999). However, as a consequence the SDM under predicts the streamwise velocity and mean shear next to a wall (Porté-Agel et al., 2000).

3.3.3. Scale-dependent dynamic model

Porté-Agel et al. (2000) extended the SDM by using the Germano identity to relate the stresses at the *primary test filter's* scale to that at a new *secondary test filter's* scale, for calculating C_S at all locations and more important, consider its variation with scale. The model is known as the Scale-Dependent Dynamic model (SDDM) and it replaces the assumption of scale invariance (Eq. (28)) with a weaker power law,

$$C_S(\alpha\widetilde{\Delta}) = \alpha^{\phi} C_S(\widetilde{\Delta}), \quad \phi \neq 0, \tag{31}$$

where α is generally an integer. A mathematical description of the SDDM is not provided here for the sake of succinctness, in short an approach similar to that of SDM but relating the stresses at three filter scales is used to obtain the value of C_S. Post-simulation analyses uncovered that not only is the value of C_S spatially variant, it is also scale-dependent with marked reductions near walls, which is consistent with increased anisotropy (see Fig. 1), thus indicating a flaw in the SDM's formulation.

In terms of computational effort, with Porté-Agel et al.'s code (see Table 1), the SDM and SDDM models require only 4% and 8% more computational time than Smagorinsky's model for simulating a neutral ABL, which is acceptable considering a marked improvement in accounting for anisotropy and scale dependence. However, the increase is marginal only because of the spectral cut-off filtering used in the code with pseudo-spectral schemes, which makes filtering an inexpensive process. Doing the same with a finite volume code will incur higher costs because of repeated filtering, which is the reason why most finite volume codes use SM or one-equation models that do not require filtering, see Moeng (1984) for example and also Table 1.

As mentioned earlier, eddy-viscosity models are purely dissipative by construction. However, simulations of a neutral ABL suggest that the SDDM is dissipative in the right amount to predict the correct velocity profile and stream-wise mean shear (Porté-Agel et al., 2000). Further, the SDDM retains its performance on coarse grids, even in regions of increased anisotropy, for example at a hill's crest (see Fig. 2). Stoll and Porté-Agel (2008) compared all the averaging schemes using the *Scale-Dependent Dynamic model*. It was noticed that the computational requirements for Lagrangian and local averaging are 22% and 8% higher than planar averaging, respectively. Additionally as an advantage, the results produced by the SDDM with Lagrangian averaging are nearly insensitive to the grid's resolution in the surface layer where most wind turbines are placed (Porté-Agel et al., 2011) (see Section 4.4).

3.4. Are SGS models physically sound?

Smagorinsky's model and its derivatives conjecture a perfect correlation between the SGS stress and the filtered strain rate. In doing so, the principal axes of the filtered strain rate tensor are assumed to be aligned with those of the subgrid tensor; DNS data does not support this assumption (Zang et al., 1993; Bardina et al., 1983). This supposed alignment produces local noise during simulations and leads to faulty predictions of local flow quantities, despite predicting mean flow quantities with reasonable accuracy (Lund, 1991).

On the other hand, Bardina et al. (1983) proposed the *Scale Similarity model* (SSM) based on experimental evidence (see Liu et al., 1994) which suggested that the smallest eddies of the filtered scales and the largest ones of the subgrid scales are similar in structure, a relation expressed mathematically as,

$$\tau_{ij} = C_B(\overline{\widetilde{u}_i\widetilde{u}_j} - \overline{\widetilde{u}}_i\overline{\widetilde{u}}_j), \tag{32}$$

where the *over-line* stands for filtering at a scale equal to or greater than that of the filter represented by *tilde* and C_B is the similarity constant.

The SSM delivers improved local statistics by removing the local noise arising from the presumed alignment of the two tensors in Smagorinsky's model (Zang et al., 1993). Additionally, the SSM can account for backscatter of energy from the dissipative scales to the inertial scales. However, this backscatter renders the model less dissipative in certain cases, which must be corrected by combining the SSM with the purely dissipative Smagorinsky's model (Mixed SSM, details in Meneveau and Katz, 2000).

Amongst all codes used for the LES studies described in this paper, only the EllipSys3D code does not use an eddy-viscosity model (Sørensen, 1995; Michelsen, 1992). Instead, it employs the *Mixed Subgrid Scale Model* (MSSM) that estimates the subgrid KE using a test filter accompanied by the assumption of *scale similarity* (Tenaud et al., 2005; Lenormand et al., 2000). The MSSM relates the subgrid stresses to the *filtered vorticity field* by means of ν_T that depends on local value of filtered vorticity (similar to how the filtered velocity field was used in Smagorinsky's model), the momentum equation for which reads,

$$\frac{\partial\widetilde{\omega}}{\partial t} - \nabla\times(\widetilde{\mathbf{u}}\times\widetilde{\omega}) = -\frac{1}{\mathrm{Re}}\nabla\times(\nabla\times\widetilde{\omega}) + \nabla\times\boldsymbol{\tau}, \tag{33}$$

where $\boldsymbol{\tau}$ is the subgrid stress and $\widetilde{\omega}$ is the filtered vorticity obtained from the filtered velocity field using,

$$\widetilde{\omega} = \nabla\times\widetilde{\mathbf{u}}. \tag{34}$$

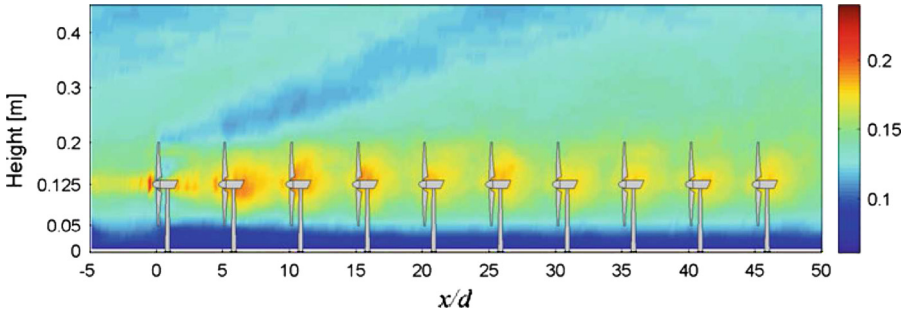

Fig. 1. A distribution of C_S determined using the Scale-Dependent Dynamic Model with Lagrangian averaging for a scaled wind farm. Reproduced from Wu and Porté-Agel (2013).

Table 1
A comparison of various LES codes for Wind Farm Simulations.

Code	SGS Model-Aver.	ABL	Time stepping	Discretisation
EllipSys3D	MSSM	Synthetic	Iterative Predictor Corrector	*Convective Term*: Blended QUICK and 4th Order CDS, *Other terms*: 2nd Order CDS
JHU-LES	SDDM-Lagrangian	Precursor LES	Adams–Bashforth	*Horizontal*: Pseudo Spectral, *Vertical*: 2nd Order Finite Difference
KULeuven	SM with Mason's function-Local	LES	Runge–Kutta	*Horizontal*: Pseudo Spectral, *Vertical*: 4th Order Energy Conserving
Porté-Agel et al.	SDDM-Lagrangian	LES	Adams–Bashforth	*Horizontal*: Pseudo Spectral, *Vertical*: 2nd Order CDS
SnS	SM with Mason's function	Synthetic	Fractional Time Stepping, *Viscous Term:* Crank–Nicolson, *Convective Term:* Adams–Bashforth	*Convective Term:* 2nd Order Face Centred, *Diffusive Term:* CDS

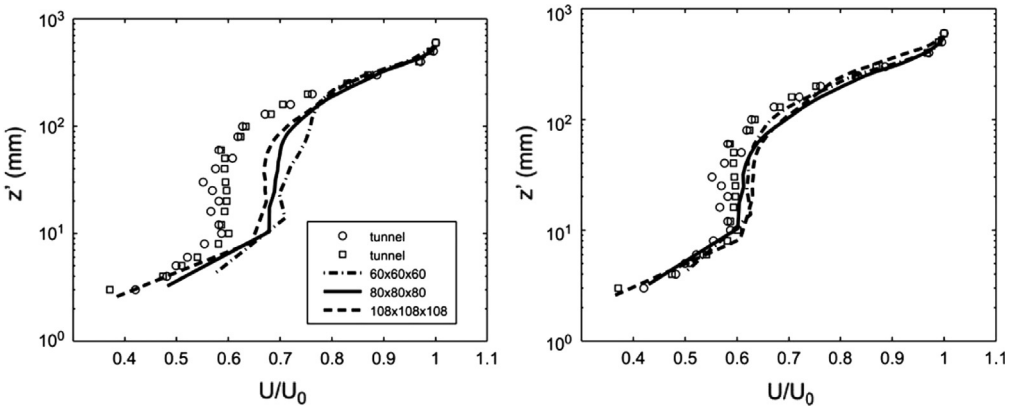

Fig. 2. A comparison of the sensitivity of the SDM (left) and the SDDM (right) in terms of the vertical profile of streamwise velocity above a hill's crest. Reproduced from Porté-Agel et al. (2011), wind tunnel data from Gong et al. (1996).

In this case, the subgrid stress is expressed as,

$$\boldsymbol{\tau} = \widetilde{\boldsymbol{u} \times \boldsymbol{\omega}} - \widetilde{\mathbf{u}} \times \widetilde{\boldsymbol{\omega}}, \tag{35}$$

and is modelled using,

$$\boldsymbol{\tau} = -\nu_T \nabla \times \widetilde{\boldsymbol{\omega}}. \tag{36}$$

The model's constants are assumed to be *scale independent* and are determined using a test filter that is twice as coarse as the grid size. As an advantage, this model is computationally less demanding and easily implementable in LES codes.

Recently, Lu and Porté-Agel (2010) introduced the *modulated gradient model* as an alternative to eddy-viscosity models. It is based on the *Taylor expansion* of the SGS stresses and the evaluation of SGS kinetic energy through the assumption of local equilibrium. LES studies have revealed that the model is capable of reproducing the log-law mean velocity profile of an ABL and the energy spectrum correctly. A distinct advantage this model offers, in addition to its accuracy, is the absence of explicit filtering, which makes the model ideal and computationally efficient for finite volume codes. Using a similar approach, Lu and Porté-Agel (2013) proposed a modulated gradient model for the scalar transport of the potential temperature. However, the model relies on the *a priori* estimation of its coefficients, just like Smagorinsky's model. A dynamic or scale-dependent dynamic formulation could reduce the dependency on *a priori* estimation, but would make the model computationally demanding for finite volume codes.

In closing, it is certain that an SGS model cannot encompass all the physics that it is required to. However, the lack of physicality in some manner, is generally compensated by the model's ability to deliver desired results. Due to the erratic nature of atmospheric flows, mean flow statistics are easier to analyse, which may have led to eddy-viscosity models being the popular choice for wind farm simulations, despite inconsistencies in their design.

4. Wind farm aerodynamics

Apart from turbulence, the turbines and the ABL must also be modelled carefully for accurate wind farm simulations. Details on turbine modelling can be found in Sanderse et al. (2011), although a relevant summary is presented here. ABL modelling will be described later in this section.

4.1. Turbine modelling for wind farm simulations

Methods for modelling wind turbines include: *actuator methods* and *direct modelling* (for CFD). Direct modelling of rotors is computationally expensive and certainly infeasible if used in combination with LES. To reduce computational costs most LES codes use the *actuator disk* (AD) and *actuator line* (AL) techniques. These methods model turbines as local volume forces that extract momentum from the flow.

The simplest approach involves implementing the axial force (or the turbine's thrust) uniformly over a disk's surface, while neglecting any tangential forces and the wake's rotation (or the AD-NR, no rotation) (Hansen, 2008; Burton et al., 2001). Although the AD-NR is computationally affordable, LES studies show that incorporating tangential forces (AD-R) and non-uniform disk loading provides a more accurate description of the wake between 5D to 7D (Porté-Agel et al., 2011).

In the AL approach, the blades are modelled as lines with forces prescribed along them. Instead of merely averaging the forces over the disk, their temporal variation is also taken into account (Sørensen and Shen, 2002). This helps resolve tip vortices correctly, which is important for detailed near wake analyses. Both methods rely on two-dimensional aerofoil data and must be corrected for tip losses (Shen et al., 2005). More details on the AD and AL approach can be found in Section 4.4.

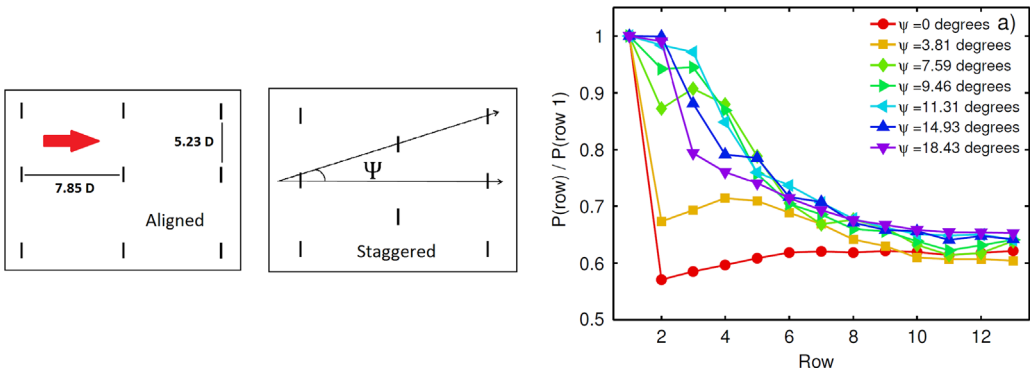

Fig. 3. Aligned: $\psi = 0^\circ$ and Staggered: $\psi = 18^\circ$ configurations of a wind farm (left and centre). The graph (right) displays the average output of various rows of wind turbines for different amounts of staggering, with maximum power around $\psi = 11^\circ$. Reproduced from Stevens et al. (2013).

LES studies are often carried out with in-house CFD codes that are summarised in Table 1. To keep the table compact, the type of grid used by the codes will be described in the text. ElliSys3D uses a Finite Volume Method to discretise the NS equations in general curvilinear coordinates. The solver is based on a block-structured multi-grid approach that solves for the primitive variables, i.e. pressure and velocity (Ivanell et al., 2008; Michelsen, 1994). In Table 1, QUICK refers to Quadratic Upstream Interpolation for Convective Kinematics (Leonard, 1979) and CDS stands for Central Discretisation Schemes (Perić and Ferziger, 2002).

Similarly, the SnS code is a non-staggered finite volume Cartesian solver in which, the equations are discretised on a collocated mesh (Armfield et al., 2002). In simulations, the computational domain is Cartesian with uniform spacing along the horizontal directions, but with a logarithmic spacing along the vertical direction to simulate the ABL more accurately (Norris et al., 2012).

On the other hand, the JHU-LES and the KULeuven code (Calaf et al., 2011), and Porte-Agel et al.s code (Porté-Agel et al., 2000), are based on the approach of using a pseudo-spectral discretisation along the horizontal direction and finite difference discretisation along the vertical direction. The reason behind this is that pseudo-spectral methods work best with periodic boundaries, which cannot represent the ground and the top of the ABL. As an exception, the KULeuven code uses a fourth-order energy-conserving discretisation (Sanderse, 2013a; Verstappen and Veldman, 2003) (also see Section 6.2), as opposed to the central second-order discretisation used by the other two. For wind farm simulations, all the codes use a computational domain with uniformly spaced grid points in all directions.

It is wise to mention that most LES studies are inter-related and many a time, the conclusions from one have been incorporated in another, which makes it difficult to classify them. Thus, in this paper, the LES investigations that have provided insight into phenomena that engineering models cannot resolve have been mentioned first, in Sections 4.2. These studies advocate the importance of proper ABL modelling for wind farm simulations, which is detailed in Sections 4.3 and 4.4. In support of what is mentioned further, a comparative analysis of various attempts to study the Horns Rev wind farm, with both LES and engineering models, is presented in Section 5.

4.2. *Wind farms: design and off-design performance*

The advantage of LES over engineering models is its ability to capture the transient evolution of turbulent eddies that are most relevant to wake development and power production. LES has enabled the study of the effect of atmospheric stratification and the presence of gusts on wake evolution and turbine loading, wake meandering etc. Further, the increase in LES studies and the results they have provided, have been conducive to the optimisation and development of LES for wind farm aerodynamics.

4.2.1. *Staggered and aligned clusters*

Two common placement strategies for large wind farms namely, staggered and aligned clusters have been the subject of various LES studies (see Fig. 3). Although, the optimisation of wind farm layouts could be done with engineering models (based on averaged power production), it is worth mentioning these LES studies as they conclude how the simple AD approach could be used for wind farm simulations with LES.

Meyers and Meneveau (2010) simulated 36 uniformly spaced (7D) wind turbines modelled as actuator disks (both AD-NR and AD-R), in staggered and aligned clusters using Smagorinsky's model with wall damping implemented in the KULeuven code. Using *Monin-Obukov's similarity theory*, the code can accurately reproduce the statistics of the ABL, without any turbines.

It was noticed that using the AD-R method to add tangential forces, only alters the normal and spanwise velocities in the far wake but not the streamwise velocity and the power produced, at high tip speed ratios and reasonable power coefficients. This finding is consistent with Troldborg's results, which indicate that the induced tangential velocity diminishes near 5D (Troldborg, 2009). Thus, the AD-NR method is suitable and faster if one aims to analyse only the power produced and if turbines are separated by at least 5D to 7D (which is the case with most modern wind farms). Staggered clusters displayed a 5% increase in power production with both AD-NR and AD-R models of the rotor because the wake is able to recover over a greater distance (twice the turbine spacing as compared to an aligned cluster). Experiments by Markfort et al. (2012) in a thermally controlled wind tunnel, confirmed the above observations for a neutral-ABL. It was also noticed that the gain is marginal if the ABL turns stable, due to the reduced entrainment of KE from the freestream.

Recently, Stevens et al. (2013) performed a similar LES study and found that completely staggering a wind farm with an originally aligned configuration, *does not* optimise the farm's efficiency (ratio of power produced to the rated power), for an inflow along the direction shown in Fig. 3. In fact, a partially staggered configuration is the most optimum one for a given aligned cluster because it minimises the number of wake-turbine interactions.

These investigations would have been tedious to conduct with engineering models, which not only tend to wrongly predict the power in case of partial wake interactions, but also for large wind

farms on which the power production is governed by the vertical exchange of momentum, which demands accurate modelling of the ABL (see Sections 5 and 4.3).

4.2.2. Turbine behaviour in off-design conditions

Churchfield et al. (2012a) performed an LES of 48, 2.3 MW turbines of the Lillgrund wind farm with Smagorinsky's model, using second-order numerical schemes constructed with the OpenFOAM toolbox (OpenFOAM, 2014). Instead of the normally used AD, AL was used to model the turbines, which costed an exorbitant *one million* processor hours. The use of AL in this case is justified as the researchers were studying the Lillgrund wind farm where the turbines are separated by a mere 4.3D, which would require proper modelling of the near wake.

Calculations followed by comparison with field data, confirmed that low streamwise spacing incurs drastic power losses owing to hindered wake development and the subsequent poor recovery of velocity deficit. This also leads to increased dynamic loading due to unmitigated turbulence intensity. Although the authors use Smagorinsky's model, they do advocate that wind farm simulations may benefit from advanced subgrid scale models, averaging schemes, more appropriate boundary conditions and local mesh adaptation. Further, they concluded that using a physical atmospheric inflow (with precursor simulation) is necessary to resolve wake meandering and the large-scale structures of the flow (1D or larger).

Lee et al. (2013) used the same code to study the effect of atmospheric instability and surface roughness on power production, wake evolution and the loads on two 5 MW NREL turbines[5] separated by 7D. Increased surface roughness leads to increased fatigue loading on the upstream turbine, whereas the effect on the downstream turbine is not as significant. The impact of atmospheric instability is weakly related to the fatigue loading but in general helps mitigate the load on downstream turbines.

With regard to power production, the downstream turbine displays better performance in an unstable ABL for a given roughness and with increasing roughness for a given stratification (Churchfield et al., 2012b). It is fair to mention that these analyses were carried out at a modest wind speed of $8\ \mathrm{ms}^{-1}$, which is below the rated speed of modern turbines.

Park et al. (2012) used Porté-Agel et al.'s LES code (see Section 3.3.3) to generate a stable ABL inflow and study the effect of surface cooling and geostrophic wind speed on turbine loading by simulating the NREL 5 MW turbine[5]. Increased surface cooling (stabler stratification) enhances the wind shear and the hub height velocity but reduces the level of turbulence. This was linked to decreased yawing and base fore-aft movement, but increased fatigue due to out-of-plane bending moments at the blade root. On the other hand, higher geostrophic wind speeds are related to increased standard deviation (fluctuations) and mean velocity at hub height but reduced wind shear, which generally increases the fatigue and maximum loading. Both these factors alter the local characteristics near the turbine and hence the loads they experience. Further, the authors advocated the use of LES to generate an accurate ABL inflow because parameters like shear, direction, speed and stability are correlated and superimposing them synthetically does not guarantee correct ABL statistics, a conclusion made by many other LES studies (Park et al., 2013).

Norris et al. (2012) used the SnS code to analyse the transient response of wakes to gusts moving through wind farms in the ABL. As opposed to steady ABL flow, in which points separated by the turbine spacing (7D) displayed little correlation, the same were shown to be strongly correlated in a gusting ABL. They noted that the response of downstream turbines to gusts and changes in blade loading in general, are dependent on the response of the upstream turbines. Based on this knowledge, the authors suggested the design of gust response controllers that may use upstream information.

The above studies clearly indicate how LES could be used to investigate the impact of atmospheric conditions on turbine loading and evaluating situations that are neglected in standard design protocols. Some of the above conclusions were also incorporated in a simple and computationally affordable Dynamic Wake meandering model by Keck et al. (2013a,b). The model yields results that are comparable to the LES-AL code used by Churchfield et al., and serves as an example of how LES can be used to improve simple mathematical models.

4.2.3. Aeroelastic coupling

Storey et al. (2012) coupled the SnS CFD code (Norris, 2000) with the FAST aeroelastic code (Jonkman and Guhl, 2005) to study the transient evolution of wakes with changes in blade loading due to atmospheric factors. Smagorinsky's model was implemented with Mason et al.'s wall damping function to reduce the value of C_S near the ground due to increased anisotropy. Validations were carried out against data from the Vindeby Offshore Wind Farm (Barthelmie et al., 2003, 2006) and the Nibe experiments (Taylor, 1990).

The coupling with FAST permitted the calculation of loads that were dynamically implemented on actuator disks to model the turbines and their wakes using CFD. It was shown that changes in blade loading affect power production and wake development, thus proving the effective coupling. Again, the authors did mention that a more accurate model of the ABL is required for a thorough analysis. More advanced SGS models could have been be employed, but were avoided in this case because the aim was to solely demonstrate if the effective coupling of CFD and BEM/loading codes is possible or not.

4.3. Wind turbine array boundary layer

When the length scale of a wind farm is much greater than that of the ABL, the flow through the wind farm develops into a fully developed *wind turbine array boundary layer* (WT-ABL), as proposed by Calaf et al. (2010). Within the WT-ABL, momentum and energy fluxes must occur vertically because the flow barely evolves spatially in the horizontal directions, instead turbulent fluxes from the faster flowing air above the farm, transfer KE into the region where the wind turbines were placed (Hamilton et al., 2012). The fluxes were observed to be equal in order of magnitude to the power extracted by the turbines, thus relating the two.

For the above, the KULeuven with Smagorinsky's model was used to collect average flow statistics, whereas the JHU-LES codes with the more advanced SDDM, was used to study the ABL profiles, being more accurate in this regard (Calaf et al., 2010). The results evinced that the interaction between the wake and the ABL must be resolved precisely for simulating large wind farms, something which has been incorporated in almost all recent LES studies.

Using their results, Calaf et al. (2010) modified Frandsen's approach of modelling the turbines as elements of surface roughness in an inflow based on two logarithmic functions (Frandsen, 1992). The new approach includes the effect of wake mixing and accounts for the reduction in the velocity at hub height due to the increased surface roughness (turbines). This is another attempt to use LES to improve simpler models by incorporating more physics, thus averting the computational requirements of LES. The

[5] A fictitious three-bladed turbine designed by NREL as reference. Details in Jonkman et al. (2009).

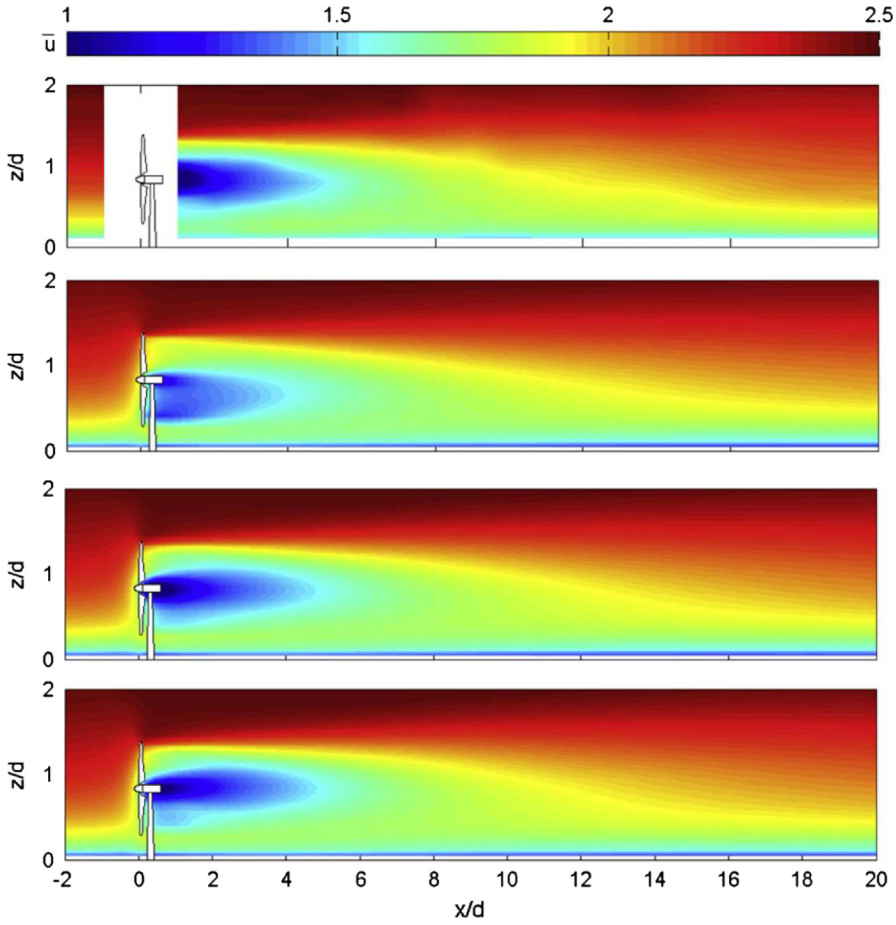

Fig. 4. Contours of time-averaged streamwise velocity on a plane perpendicular to the turbine's plane, located at the turbine's centre line (from top to bottom: wind tunnel data, AD-NR, AD-R and AL). Reproduced from Porté-Agel et al. (2011).

modified Frandsen's model was later used by Meyers and Meneveau (2012) to devise a strategy for placing wind turbines within a fully developed wind farm boundary layer (neutral) over a smooth terrain, so as to optimise the power output. However, the effects of yawed inflow and the distinction between spanwise and streamwise spacing were ignored.

Meyers and Meneveau (2013) also used the LES data to study the fluxes of mass, momentum and kinetic energy by visualising them as *transport tubes* and discerned that the path taken while transporting these variables, depends on the turbine placement and spacing. Recent experiments on scaled wind farms suggest that turbulent structures of order of 1D are mainly responsible for the vertical entrainment of KE. The difference in coherence among these structures between the top and the bottom of the wake is what drives the KE flux. Once the flow has developed along the streamwise direction, it is this flux that helps the wakes recover faster than their upstream counterparts (Hamilton et al., 2012).

Recently, Abkar and Porté-Agel (2013) studied the effect of atmospheric stability on the entrainment of energy from the flow above the wind farm. Increased stability leads to lesser entrainment and reduced boundary layer height, hence reduced power production. Based on their observations, they modified Frandsen's neutral ABL based formula, for use with a stable ABL.

Finally as application of LES, the codes were modified to incorporate atmospheric stability to study the effects of the WT-ABL on the vertical mixing of heat and moisture. Following discordance between meteorological surveys and laboratory experiments, it was finally concluded that a wind farm's presence increases the scalar fluxes from the surface in a neutral ABL and that the change is weakly dependent on the turbines' spacing and thrust coefficients (Calaf et al., 2011).

4.4. Simulations of scaled wind farms

Porté-Agel et al. (2011) used the SDDM for solving the filtered NS equations, in combination with *Boussinesq's approximation* and transport equation for the potential temperature to simulate the ABL (see Table 1). The code was also used to simulate scaled wind turbines and wind farms. Instead of using data from field experiments, data from high resolution anemometry based wind tunnel experiments on scaled turbines was used for validating the code (Chamorro and Porté-Agel, 2011, 2009). The wind tunnel could mimic conditions that exist in the ABL under every stratification (Chamorro and Porté-Agel, 2010; Zhang et al., 2013).

Despite the low Reynolds number, the detailed data could help validate LES-ABL models. Attempts to simulate the wind tunnel experiments with LES led to important conclusions that helped suggest a suitable framework for LES of wind farms (Porté-Agel et al., 2010). It was observed that AD-NR with a uniformly loaded rotor in spite of being speedy, is not completely accurate and will lead an under prediction in the wake's velocity deficit and the turbulence intensity at the turbine's top-tip level till 5–7 D (see Fig. 4).

Using a non-uniformly loaded AD with both axial and tangential forces to account for the wake's rotation, or the AD-R, is a wise alternative to using the computationally expensive AL technique, which is more suitable for near wake analyses (Porté-Agel et al., 2011). Grid-sensitivity tests revealed that the AD-R method can be

used by placing no more than 5 and 7 grid points on the disk along the spanwise and vertical directions (Wu and Porté-Agel, 2011), respectively, placing more points does not improve the results significantly (for neutral ABL only).

4.5. Atmospheric boundary layer

Most LES studies have clearly concluded that the proper modelling of the ABL is necessary for correct predictions with LES codes. This section describes how an LES generated ABL is more accurate than a synthetically generated ABL.

4.5.1. Synthetic inflow

For the simulations that were done with the EllipSYS3D code, the synthetic ABL was implemented in two steps. First, a mean shear is specified across the domain as a distribution of volume forces. Next, the turbulence intensity is set at the inflow boundary, again by means of volume forces. These forces are calculated from three-dimensional velocity fluctuations prescribed by Mann (1994, 1998), to generate a turbulent field that is anisotropic and incompressible.

The Immersed Boundary Method (IBM) is used to introduce the mean shear on which the data from the turbulence field is superimposed. However, the turbulence would tend to decay till the region of interest (wind turbines), which is generally at a considerable distance from the inflow boundary. To correct this, Troldborg et al. (2013); Keck et al. (2013c) used the IBM to specify the turbulent fluctuations in a plane close to the turbines. Comparisons with field data revealed that the turbulence characteristics in the wake of a single turbine are well resolved using this approach.

It is important to note that using a synthetic ABL inflow hinges on the assumption that the mean shear and turbulence statistics can be specified independently. This is contrary to recent conclusions by detailed LES studies that the two parameters are highly correlated (see Section 4.2.2). Although the results obtained with this method compare well with field data from tests on single turbines, it might not be effective for a wind farm simulation that relies on the interaction between the wake and the ABL and hence its accurate modelling (see Section 5).

4.5.2. LES generated ABL

The classic ABL is simulated using *Monin-Obukov's similarity theory* to ascribe the wall stress to the first grid point above the ground, following which the boundary layer is allowed to develop in course of the simulation. Although Monin-Obukov's formulation is meant for mean flow variables (Porté-Agel et al., 2000; Businger et al., 1971) and hence suitable for RANS, it has been used for LES due to the lack of an alternative approach (Moeng, 1984).

However, simulating the ABL is not straightforward. After introducing the SDDM (Porté-Agel et al., 2000), various studies on SGS modelling were carried out to demonstrate the importance of high-order SGS modelling for generating an ABL-like flow. An important conclusion was the dependence of C_S on scale, its reduction near the ground due to increased anisotropy and reduced characteristic length scales (especially in regions of large mean shear) and its increase near the wake's centre line due to reduced anisotropy (Wu and Porté-Agel, 2011; Wan and Porté-Agel, 2011). Thus, using an SGS model that incorporates these effects is important to simulate the turbulence correctly throughout the computational domain.

The SDDM relies on averaging schemes to avert numerical instability (see Section 3.3.2), which must be chosen wisely in the presence of wind turbines. For an ABL developing over a homogeneous terrain and in the absence of wind turbines, planar averaging should be sufficient. However, in presence of surface inhomogeneities and wind turbines, Local and Lagrangian averaging are more appropriate (Wan et al., 2007). In fact, Lagrangian averaging along path lines and even local averaging renders the model's coefficients self consistent. The flow's statistics like wind speed, potential temperature, momentum and buoyancy fluxes are then less sensitive to grid resolution in the lower 10% of the ABL (surface layer), where the turbines are placed (Stoll and Porté-Agel, 2008).

Further, for simulating an ABL of height H, over an area H^2, a 128^3 grid would suffice and generate results similar to those produced by a 192^3 grid (Beare et al., 2006), with the SDDM-Lagrangian averaging (Stoll and Porté-Agel, 2008). A lower resolution like 64^3 would also be reasonably accurate. Local averaging on the other hand, requires high grid resolution and planar averaging is not capable of rendering the ABL correctly even at 128^3.

Finally, a scale dependent dynamic model for solving the filtered transport equation for the potential temperature was also proposed by Porté-Agel (2004). This permitted the simulation of non-neutral stratifications of the ABL (Basu and Porté-Agel, 2006) and also the investigation of their effects on wake development. For LES studies on stable and convective ABLs, the readers are referred to Lu and Porté-Agel (2011) and Porté-Agel et al. (2014), respectively. Readers may also refer to Chamorro and Porté-Agel (2010) and Zhang et al. (2013) for an experimental insight into the effects of ABL stratification.

5. Simulations of the horns rev wind farm

The Horns Rev wind farm in Denmark has been simulated with both engineering models and LES. The two LES studies that will be compared in this section, are those by Ivanell and Stevens et al. For the sake of simplicity, the individual results are not shown here, but can be found in Ivanell (2009), Stevens et al. (2013, 2014) and Barthelmie et al. (2009) (for engineering models). However, Fig. 5 compares the results obtained with engineering models and LES codes against field data from the Horns Rev wind farm. Schepers (2012) presents a detailed discussion on the performance on engineering models.

Ivanell (2009) simulated two rows of the Horns Rev wind farm with the EllipSYS3D (see Table 1) code using periodic boundaries, in effect simulating an infinitely large cluster of turbines. A distribution of volume forces was used to generate a synthetic ABL inflow (see Section 4.5.1) and the turbines were represented by actuator disks. The code under predicted the power produced

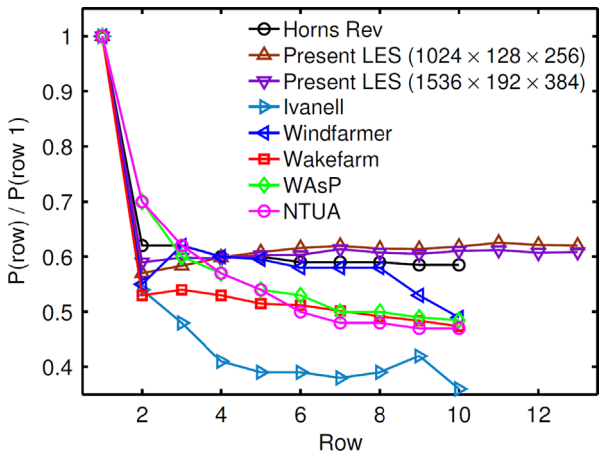

Fig. 5. Average power output of downstream turbines at the Horns Rev wind farm, obtained with engineering models and LES codes. Reproduced from Stevens et al. (2013).

by a downstream turbine in case of a full wake interaction. A partial wake interaction on the other hand, led to over prediction. After averaging the power predictions over inflow angles in a range of 30°, engineering models were noticed to yield better results.

Recently, Stevens et al. (2013, 2014) used the JHU-LES code to simulate the entire wind farm. Instead of a synthetic ABL, a precursor method was used to simulate the ABL and concomitantly feed the developing flow as an inflow condition for the wind farm simulation. In addition, the JHU-LES uses high-order SGS models and numerics (see Table 1). A better correlation with field data averaged over 30° was obtained, which was attributed to improved ABL modelling. It was noticed that most engineering models performed well with aligned or nearly aligned wind farm configurations leading to full wake interactions. Staggering of turbines by more than 5° leads to a decline in correlation because of increased partial wake interactions.

At the same time, for a perfectly aligned configuration the engineering models were not able to predict the power production after the fourth row as accurately as JHU-LES (Barthelmie et al., 2009). A possible explanation is that following multiple full-wake interactions, the wind farm behaves nearly as a fully developed WTA-BL (see Section 4.3) and power production is then dominated by vertical exchange of kinetic energy with the faster atmospheric freestream. In such a situation, it is imperative to model the interaction between the ABL and the wakes correctly, something which engineering models despite tuning, might not be able to achieve. On the other hand, the JHU-LES code with a precursor LES-ABL simulation is capable of reproducing these interactions correctly.

Although the improved results were attributed to a more physical description of the ABL, the authors would like to emphasise that the LES studies differed in other aspects like SGS modelling, numerical schemes and more important, the grid resolution. Stevens et al. used a significantly higher grid resolution, that only improved the accuracy, but also reduced the dependence on the SGS model and its ability to incorporate more physics in the LES code.

In such a situation, it is difficult to confirm which of the three, SGS model, grid resolution or ABL specification, is most conducive to an accurate LES. Only a detailed comparative study of LES codes on wind farms, like those performed by Porté-Agel et al. (see Section 4.4) on the ABL, can provide an answer to the above.

6. Numerics

The previous sections enlist the contributions of LES to wind farm aerodynamics and how improvements in SGS modelling have made it indispensable for not only the simulation of wind farms, but to also enhance simple engineering models. It is obvious that an SGS model alone does not dictate the accuracy and efficiency of LES codes. Other aspects like spatio-temporal discretisation and boundary conditions must be considered.

A detailed discussion of these parameters with regard to LES, is beyond the scope of this paper. Further, it is hard to conclude what discretisation schemes and boundary conditions are most suitable for the LES of wind farms due to the absence of comparative studies. However, this section describes certain features that would be desirable for LES.

6.1. Boundary conditions

A typical computational domain used in for the LES of wind farms in shown in Fig. 6.

Generally the upper boundary is assigned a stress free condition (Porté-Agel et al., 2000) or a prescribed shear condition (Jiménez et al., 2007), as long as the height of the domain is greater than that of the turbine. At times, a symmetry condition (zero normal velocity and normal gradients) has also been used, but this can be erroneous for WT-ABL simulations that rely on the vertical exchange of momentum and energy (see Section 4.3).

From Table 1, one can surmise that most LES codes are based on pseudo-spectral methods for resolving the flow in the horizontal direction, which unfortunately would require Periodic Boundary Conditions in streamwise and spanwise directions (although Spectral formulations for non-periodic boundaries are known). This periodicity permits the simulation of fully developed wind farms or a row of wind turbines deep within the WT-ABL, as done by Ivanell, without requiring a large domain (Calaf et al., 2011; Ivanell, 2009). When periodic conditions are used, the flow must be forced artificially through the domain with a constant pressure gradient or driven by a geostrophic wind (Catalano and Moeng, 2010). This can however be avoided with a precursor ABL simulation, which also provides a more physically sound rendition of the ABL (see Section 5).

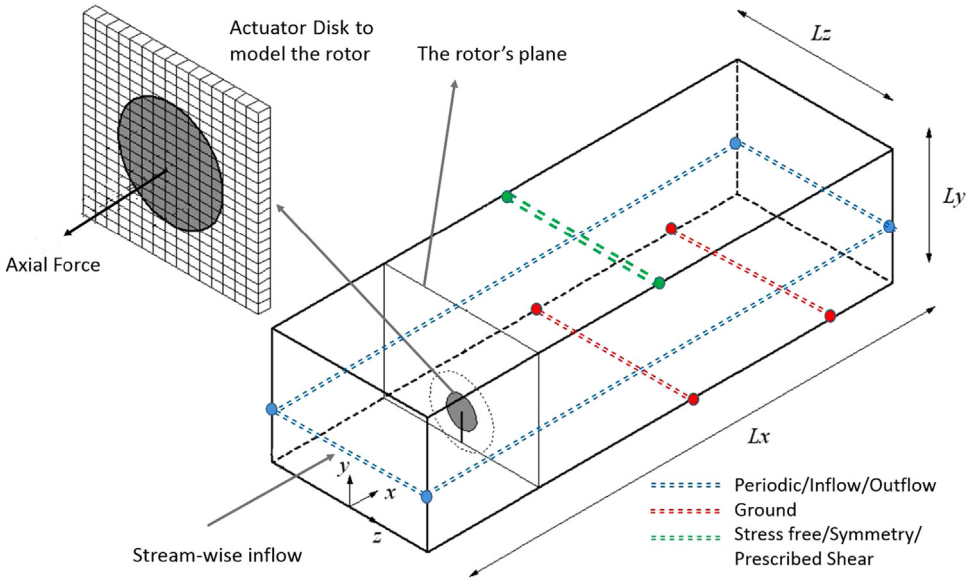

Fig. 6. An example of a computational domain for simulating wind farms. Adapted from Jiménez et al. (2007).

A framework comprising the finite difference based Weather Research and Forecasting (WRF) model and the coupled OpenFOAM-FAST solver (see Sections 4.2.2 and 4.2.3) has also been proposed (Churchfield et al., 2013). The intention is to use WRF to provide more appropriate boundary conditions for the LES of wind farms. Such a coupling could permit the simulation of extreme events like gusts or changes in wind speed and direction over a large wind farm, and also help analyse the effect of large wind farms on local weather.

6.2. Discretisation schemes

LES is more adept at preserving large scale structures over distances between successive turbines due to the more accurate definition of turbulence that it provides. But most wind farm simulations are done on coarse grids, which may lead to immoderate numerical errors with certain discretisation schemes. RANS based codes are stabilised with upwind schemes that bring along artificial numerical dissipation, and more so on coarse grids. If left unchecked, numerical dissipation (even through temporal schemes), even in a small amount, can spuriously dampen large scale structures (Sagaut, 2006). As for wind farm simulations, artificial dissipation leads to a quicker recovery of the wake i.e. an under-prediction of the velocity deficit at all locations downstream of a turbine (Cabezón et al., 2011).

To come to terms with numerical stability and dissipation, EllipSys3D uses a blend of central and upwind schemes. However, using a central scheme can lead to dispersion, which in simple terms would mean that a wake is being transported correctly, although its velocity field is distorted with wiggles. Similarly, the simulations with OpenFOAM (see Section 4.2.2) used a second-order central scheme that would also have led to dispersion. However, this was done in combination with Smagorinsky's model that is dissipative enough for smoothing most wiggles. On the other hand, high-order spectral methods can combat these effects but are computationally demanding, yet common in LES codes. Energy-conserving schemes that are free from numerical dissipation could be a fine alternative (Verstappen and Veldman, 2003). Initially named as *Symmetry-Preserving schemes*, they ensure the conservation of kinetic-energy, which is an invariant property of incompressible flows, and hence are also known as energy-conserving schemes. Unfortunately, the numerical dissipation is averted through the use of central-differences, which as drawback incurs numerical dispersion, hence requiring a dissipative SGS model. Although this can be remedied with higher-order discrete operators, the boundary treatment becomes challenging (Sanderse, 2013a, 2011).

One must also ensure that the temporal discretisation introduces minimal dissipation, especially if the temporal averaging is used to process data. Although most codes use high-order schemes, none a them are free from numerical dissipation, which consequently demands the restriction of the time step to avoid impacting the large scales, even with implicit methods (Bechmann, 2006). With energy-conserving methods, the time step could be made relatively larger reducing the computational time (Sanderse, 2013b). However, the benefits of such a scheme are curbed by the dispersive errors, the presence of boundaries that could lead to an overall reduction in accuracy and the loss of numerical stability (ref. Sanderse et al., 2011 and references therein).

7. Summary

The following points summarise Section 4:

- Wind farms simulations have been performed predominantly with eddy-viscosity models (except for the MSSM in EllipSYS3D). Even the simple Smagorinsky's model is sufficient for qualitative analyses of wind farm aerodynamics. But for accuracy, researchers must rely on more advanced SGS models.
- With proper ABL modelling, LES can help assess the performance of wind farms in off-design conditions like non-neutral ABLs and gusts. Effective coupling with aeroelastic codes could provide great insight into turbine loading in such situations.
- Wind farm simulations rely on accurate wake-ABL interaction, which is possible only with a correct ABL model. This is of great consequence for simulating large wind farms on which the ABL evolves into a WT-ABL. Generating a synthetic ABL requires lesser computational effort than precursor simulations with LES, but lacks the statistical correlations that exist in a physical ABL.
- Using the SDDM with Lagrangian averaging generates an ABL that is accurate enough for wind farm simulations, but is computationally expensive. Nonetheless, it retains its precision even on coarse grids making it suitable for LES.
- From simulations of the Horns Rev wind farm, it is apparent that the performance of engineering models is comparable to that of certain LES codes, as far as generating averaged statistics. When done with accurate ABL modelling and with advanced SGS models, on relatively refined grids, LES delivers a substantially better performance.
- LES data can be utilised to enhance simple engineering models to retain computational efficiency but ensuring better accuracy.
- Numerical schemes for LES must ensure zero numerical dissipation for high accuracy. Pseudo-spectral and Energy-Conserving spatial discretisation schemes are useful in this regard, the latter however requires a higher-order formulation to be as accurate as the former. Additionally, energy-conserving time integration with zero dissipation would help speed up computations, but requires further modifications to avert loss in accuracy and stability.
- A stress-free upper boundary is most appropriate for wind farm simulations. Periodic boundaries required by spectral schemes can be avoided with Energy-Conserving schemes, which are however not as accurate as the former.
- SGS models have been compared in terms of their ability to simulate the ABL (see Section 3.3.3). It is clear that above beyond a certain resolution, the effect of the SGS model on the ABL's is nullified and even a simple model is sufficient for an ABL simulation. However, such a conclusion with regard to wind farm simulations is yet to be drawn.

8. Discussion

LES's capacity to consolidate more physics than engineering models has enabled detailed investigations of wind farm aerodynamics. Researchers have gained insight into the effects of ABL stratification, wake meandering, gusts etc. on power production, wake evolution and fatigue loading, even on large wind farms. Although today's computational resources are not sufficient to replace engineering models with LES, the knowledge gained through LES can help enhance engineering models, while preserving their speediness and simplicity, which make them favourable.

Despite their speed and acceptable accuracy, engineering models demand pre-tuning with data from wind tunnel or field experiments. Controlled wind tunnel tests provide reliable data albeit at low Reynolds numbers. Nonetheless, the data is reliable for assessing the numerical aspects of LES like SGS modelling, numerical schemes etc. Field data encompasses the exact operating conditions and is suitable for validating wind turbine/farm

simulations, but is generally inadequate. Further, field data at times, could bear a high standard deviation given the erratic nature of the atmosphere, which may compromise the data's reliability. Thus, despite careful tuning, most engineering models cannot deliver dependable data for very large wind farms or inflow angles involving high number of wake interactions etc. As an alternative, the comprehensive and high-fidelity aerodynamic data generated with an LES code could be used for tuning engineering models. This tactic could prove fruitful but has yet to be looked into. Researchers have modified Frandsen's model and even proposed a simple but effective model for wake meandering. Similarly, LES generated transfer functions could be built into engineering models to account for or to improve the modelling of atmospheric stability, detailed wake-ABL interactions especially on large wind farms, effects of gusts to name a few.

Concerning LES, it is certain that no SGS model is complete and their efficacy is situation-dependent. Smagorinsky's model and its derivatives are popular being easily implementable and capable of producing good data on wind farm aerodynamics, despite their assumptions lacking conclusive evidence. On the other hand, Scale Similarity models (apart from MSSM in Ellip-SYS3D) have not been applied to wind farm simulations. These models would be worth exploring, not as an alternative but to complement eddy-viscosity models through linear combination for instance, to assimilate more physics. However, Scale Similarity models could become computationally expensive, especially with Finite Volume methods because of explicit filtering. As an alternative, one could employ the modulated gradient model, which is quite accurate at simulating the ABL, but unfortunately relies on good *a priori* estimation of its coefficients. Ultimately, it is certain that better ABL and SGS modelling are contributory to accurate results on coarse grids, which are common in practice.

Regarding coarse grids, it would be wise to develop numerical schemes instead of relying on excess computational power. LES codes cannot count on upwind schemes of stability because the numerical dissipation will dampen the resolved scales, more so on coarse grids. High-order spectral methods are thus common in LES but are computationally expensive. On the other hand, Energy-conserving schemes are free from numerical dissipation and permit the use of non-periodic boundaries, but require further investigation at this stage. In terms of boundary conditions, Monin-Obukov's approach remains the only option for modelling the ABL, despite being deemed unsuitable for LES. Lately research has been focussed on developing a more appropriate technique that could be adapted for inhomogeneous terrains, but experiments would be more instrumental in enhancing the existing approach.

Comparative studies of LES codes by individually assessing the importance and impact of each of the above parameters are required. This can be extrapolated to another facet that needs immediate attention, which is quantification of errors in LES. Although much is known about the interplay between SGS modelling and grid resolution for ABL simulations, similar knowledge in terms these parameters along with rotor modelling, numerical schemes etc., for wind farms simulations is lacking. Such investigations will be computationally expensive, particularly with grid-refinement studies, however would be conducive to the optimisation of LES codes.

In closing, LES studies with different codes have used different field/experimental data for validation, making it difficult (using literature alone) to assess their competency in simulating wind farms. This should provide impetus towards the collection of quality field/experimental data that could serve as a benchmark validation case.

Acknowledgement

This paper was prepared under the aegis of the Ph.D. research organised by the Marie Curie Initial Training Networks's project MARE-WINT (new MAterials and REliability in offshore WINd Turbines technology), which is funded by the European Commission as part of the Seventh Framework Programme under the Grant Agreement numbered 309395. MARE-WINT's contribution is much acknowledged.

References

Abkar, M., Porté-Agel, F., 2013. The effect of free-atmosphere stratification on boundary-layer flow and power output from very large wind farms. Energies 6, 2338–2361.

Abramovich, G.N., 1963. The Theory of Turbulent Jets, 1st ed. MIT Press, Cambridge, MA.

Ainslie, J.F., 1985. Development of an Eddy viscosity model for wind turbine wakes. In: Proceedings of the 7th BWEA Wind Energy Conference, Oxford, pp. 61–66.

Ainslie, J.F., 1998. Calculating the field in the wake of wind turbines. J. Wind Eng. Ind. Aerodyn. 21, 213–224.

Ammara, I., Leclerc, C., Masson, C., 2002. A viscous three-dimensional differential/actuator disk method for the aerodynamic analysis of wind farms. J. Solar Eng. 124, 345–356.

Armfield, S., Norris, S., Morgan, P., Street, R., 2002. A parallel non-staggered Navier–Stokes solver implemented on a workstation cluster. In: Computational Fluid Dynamics 2002: Proceedings of the Second International Conference on Computational Fluid Dynamics, Sydney, Australia.

Bardina, J., Ferziger, J.H., Reynolds, W.C., 1983. Improved Turbulence Models Based on Large Eddy Simulation of Homogeneous, Incompressible, Turbulent Flows (Ph.D. thesis). Department of Mechanical Engineering, Stanford University.

Barthelmie, R., Folkerts, L., Ormel, F., Sanderhoff, P., Eecen, P., Stobbe, O., Nielsen, N., 2003. Offshore wind turbine wakes measured by sodar. J. Atmosph. Oceanic Technol. 20, 466–477.

Barthelmie, R., Larsen, G., Pryor, S., Jørgensen, H., Bergström, H., Schlez, W., Rados, K., Lange, B., Vølund, P., Neckelmann, S., Mogensen, S., Schepers, G., Hegberg, T., Folkerts, L., Magnusson, M., 2004. ENDOW (Efficient development of offshore wind farms): modelling wake and boundary layer interactions. Wind Energy 7, 225–245.

Barthelmie, R., Folkerts, L., Larsen, G., Rados, K., Pryor, S., Frandsen, S., Lange, B., Schepers, G., 2006. Comparison of wake model simulations with offshore wind turbine wake profiles measured by sodar. J. Atmosph. Oceanic Technol. 23, 888–901.

Barthelmie, R.J., Frandsen, S.T., Réthoré, P.E., Jensen, L., 2007. Analysis of the atmospheric impacts on the development of wind turbine wakes at the Nysted wind farm. In: European Offshore Wind Conference, Berlin.

Barthelmie, R.J., Frandsen, S.T., Hansen, K., Schepers, J.G., Rados, K., Schelz, W., Neubert, A., Jensen, L.E., Neckelmann, S., 2009. Modelling the impact of wakes on power output at Nysted and Horns Rev. In: European Wind Energy Conference, Marseille.

Bastankhah, M., Porté-Agel, F., 2014. A new analytical model for wind-turbine wakes. Renew. Energy 70, 116–123.

Basu, S., Porté-Agel, F., 2006. Large-Eddy simulation of stably stratified atmospheric boundary layer turbulence: a scale-dependent dynamic modeling approach. J. Atmosph. Sci. 63, 2074–2091.

Beare, R.J., Macvean, K.M., Holtslag, A.A.M., Cuxart, J., Esau, I., Golaz, J.C., Jimenez, M. A., Khairoutdinov, M., Kosovic, B., Lewellen, D., Lund, T.S., Lundquist, J.K., Mccabe, A., Moene, A.F., Noh, Y., Raasch, S., Sullivan, P., 2006. An intercomparison of large-Eddy simulations of the stable boundary layer. Boundary-Layer Meteorol. 118, 247–272.

Bechmann, A., 2006. Large-Eddy Simulation of Atmospheric Flow over Complex Terrain (Ph.D. thesis). Department of Wind Energy, Risø National Laboratory - Technical University of Denmark.

Boussinesq, J.V., 1877. Essai sur la Théorie des Eaux Courantes (in French). Mémoires présentés par divers savants à l'Académie des Sciences, Paris 23, 1–680.

Bou-Zeid, E., Meneveau, C., Parlange, M., 2005. A scale-dependent Lagrangian dynamic model for large Eddy simulation of complex turbulent flows. Phys. Fluids 17, 025105.

Burton, T., Sharpe, D., Jenkins, N., Bosanyi, E., 2001. Wind Energy Handbook. John Wiley & Sons, Chichester.

Businger, J.A., Wyngaard, J.C., Izumi, Y., Bradley, E.F., 1971. Flux-profile relationships in the atmospheric surface layer. J. Atmosph. Sci. 28, 181–189.

Cabezón, D., Migoya, E., Crespo, A., 2011. Comparison of turbulence models for the computational fluid dynamics simulation of wind turbine wakes in the atmospheric boundary layer. Wind Energy 14, 909–921.

Calaf, M., Meneveau, C., Meyers, J., 2010. Large eddy simulation study of fully developed wind-turbine array boundary layers. Phys. Fluids 22, 015110.

Calaf, M., Parlange, M.B., Meneveau, C., 2011. Large eddy simulation study of scalar transport in fully developed wind-turbine array boundary layers. Phys. Fluids 23, 126603.

Catalano, F., Moeng, C., 2010. Large-Eddy simulation of the daytime boundary layer in an idealized valley using the weather research and forecasting numerical model. Boundary-Layer Meteorol. 137, 49–75.
Chamorro, L.P., Porté-Agel, F., 2009. A wind tunnel investigation of wind turbine wakes: boundary layer turbulence effects. Boundary-Layer Meteorol. 132, 129–149.
Chamorro, L.P., Porté-Agel, F., 2010. Effects of thermal stability and incoming boundary-layer flow characteristics on wind-turbine wakes: a wind-tunnel study. Boundary-Layer Meteorol. 136, 515–533.
Chamorro, L.P., Porté-Agel, F., 2011. Turbulent flow inside and above a wind farm: a wind tunnel study. Energies 4, 1916–1936.
Churchfield, M., Lee, S., Moriarty, P., Martínez, L., Leonardi, S., Vijayakumar, G., Brasseur, J., 2012a. A large-Eddy simulation of wind-plant aerodynamics. In: 50th AIAA Aerospace Sciences Meeting Including the New Horizons Forum and Aerospace Exposition, Nashville, Tennessee.
Churchfield, M., Lee, S., Michalakes, J., Moriarty, P., 2012b. A numerical study of the effects of atmospheric and wake turbulence on wind turbine dynamics. J. Turbulence 13, 1–32.
Churchfield, M.J., Michalakes, J., Vanderwende, B., Lee, S., Sprague, M.A., Lundquist, J.K., Moriarty, P.J., 2013. Using Mesoscale Weather Model Output as Boundary Conditions for Atmospheric large-Eddy Simulations and Wind-plant Aerodynamic Simulations. Technical Report PR-5000-61122, National Renewable Energy Laboratory, Colorado, USA.
Cleijne, J.W., 1993. Results of the Sexbierum Wind Farm Single Wake Measurements. Technical Report TNO-93-082, TNO Institute of Environmental and Energy Technology, The Netherlands.
Crespo, A., Hernández, J., 1993. Analytical correlations for Turbulence characteristics in the Wakes of Wind Turbines. In: Proceedings of the 1993 European Wind Energy Conference. Travenmünde, Germany, pp. 436–439.
Crespo, A., Hernández, J., 1996. Turbulence characteristics in Wind Turbine Wakes. J. Wind Eng. Ind. Aerodyn. 6, 71–85.
Crespo, A., Manuel, F., Moreno, D., Fraga, G., Hernández, J., 1985. Numerical analysis of wind turbine wakes. In: Proceedings of the Delphi Workshop on Wind Energy Applications, Delphi, Greece, pp. 15–25.
Crespo, A., Hernández, J., Frandsen, S., 1999a. Survey of modelling methods for wind turbine wakes and wind farms. Wind Energy 2, 1–24.
Crespo, A., Frandsen, S., Gómez-Elvira, R., Larsen, S.E., 1999b. Modelization of a large wind farm, considering the modification of the atmospheric boundary layer. In: Proceedings of the 1999 European Union Wind Energy Conference, Nice, France.
Davidson, P.A., 2004. Turbulence – An Introduction for Scientists and Engineers. Oxford University Press, Oxford.
Elliot, D.L., 1991. Status of wake and array loss research. In: Windpower Conference, Palm Springs, California.
Foias, C., Manley, O., Rosa, R., Temam, R., 2001. Navier–Stokes Equations and Turbulence, 1st ed. Cambridge University Press, Cambridge.
Frandsen, S., 1992. On the wind speed reduction in the center of large clusters of wind turbines. J. Wind Eng. Ind. Aerodyn. 39, 251–265.
Frandsen, S., Barthelmie, R., Pryor, S., Rathmann, O., Larsen, S., Højstrup, J., Thøgersen, M., 2006. Analytical modelling of wind speed deficit in large offshore wind farms. Wind Energy 9, 39–53.
Frisch, U., 1995. Turbulence, the Legacy of A.N. Kolmogorov. Cambridge University Press, Cambridge.
Germano, M., 1986. A proposal for a redefinition of the turbulent stresses in the filtered Navier–Stokes equations. Phys. Fluids 29, 2323–2324.
Germano, M., 1987. On the non-Reynolds averages in turbulence. In: 19th AIAA Fluid Dynamics, Plasma Dynamics, and Lasers Conference, Honolulu, Hawaii.
Germano, M., 1992. Turbulence: the filtering approach. J. Fluid Mech. 238, 325–336.
Germano, M., Piomelli, U., Moin, P., Cabot, W.H., 1991. A dynamic subgrid-scale Eddy viscosity model. Phys. Fluids A: Fluid Dyn. 3, 1760–1765.
Geurts, B.J., 2004. Elements of Direct and Large-Eddy Simulation. Edwards, Cheltenham.
Ghosal, S., 1999. Mathematical and physical constraints on large-Eddy simulation of turbulence. AIAA J. 37, 425–433.
Gómez-Elvira, R., Crespo, A., Migoya, E., Manuel, F., Hernández, J., 2005. Anisotropy of turbulence in wind turbine wakes. J. Wind Eng. Ind. Aerodyn. 93, 797–814.
Gong, W., Taylor, P.A., Dörnbrack, A., 1996. Turbulent boundary-layer flow over fixed aerodynamically rough two-dimensional sinusoidal waves. J. Fluid Mech. 312, 1–37.
Grindstein, F.F., Margolin, L.G., Rider, W.J., 2007. Implicit Large Eddy Simulation: Computing Turbulent Fluid Dynamics, 1st ed. Cambridge University Press, Cambridge.
Hamilton, N., Kang, H., Meneveau, C., Cal, R., 2012. Statistical analysis of kinetic energy entrainment in a model wind turbine array boundary layer. J. Renew. Sustain. Energy 4.
Hansen, M.O.L., 2008. Aerodynamics of Wind Turbines, 2nd ed. Earthscan, London.
Hansen, M.O.L., Sørensen, J.N., Voutsinas, S., Sørensen, N., Madsen, H.A., 2006. State of the art in wind turbine aerodynamics and aeroelasticity. Prog. Aerosp. Sci. 42, 285–330.
Horiuti, K., 1993. A proper velocity scale for modeling subgrid-scale eddy viscosities in large Eddy simulation. Phys. Fluids A: Fluid Dyn. 5, 146–157.
Ivanell, S., 2009. Numerical Computations of Wind Turbine Wakes (Ph.D. thesis), Department of Mechanics, Royal Institute of Technology, Stockholm, Sweden.
Ivanell, S., Mikkelsen, R., Sørensen, J.N., Henningson, D., 2008. Validation of Methods Using EllipSys3D. Technical Report TRIRA-MEK 2008:12, Royal Institute of Technology, Sweden.
Jensen, N.O., 1983. A Note on Wind Generator Interaction. Technical Report Risø-M-2411, Risø National Laboratory, Roskilde, Denmark.
Jensen, L.E., Mørch, C., Sørensen, P.B., Svendsen, K.H., 2004. Wake Measurements from the Horns Rev Wind Farm. In: European Wind Energy Conference, London.
Jiménez, Á., Crespo, A., Migoya, E., Garcia, J., 2007. Advances in large-Eddy simulation of a wind turbine wake. J. Phys. Conf. Ser. 75, 012041.
Jonkman, J.M., Guhl, M.L., 2005. FAST Users' Guide, Technical Report EL-500-38230, NREL.
Jonkman, J., Butterfield, S., Musial, W., Scott, G., 2009. Definition of a 5-MW Reference Wind Turbine for Offshore System Development. Technical Report TP-500-38060, National Renewable Energy Laboratory, Colorado.
Keck, R.-E., de Maré, M., Churchfield, M.J., Lee, S., Larsen, G., Madsen, H.A., 2013a. On atmospheric stability in the dynamic wake meandering model. Wind Energy. URL http://dx.doi.org/10.1002/we.1662.
Keck, R.-E., de Maré, M.J., Churchfield, M., Lee, S., Larsen, G., Madsen, H.A., 2013b. Two improvements to the dynamic wake meandering model: including the effects of atmospheric shear on wake turbulence and incorporating turbulence build-up in a row of wind turbines. Wind Energy. URL http://dx.doi.org/10.1002/we.1686.
Keck, R.-E., Mikkelsen, R., Troldborg, N., de Maré, M., Hansen, K.S., 2013. Synthetic atmospheric turbulence and wind shear in large Eddy simulations of wind turbine wakes. Wind Energy. URL http://dx.doi.org/10.1002/we.1631.
Lee, S., Churchfield, M., Moriarty, P., Jonkman, J., Michalakes, J., 2013. A numerical study of atmospheric and wake turbulence impacts on wind turbine fatigue loadings. J. Solar Energy Eng. Trans. ASME 135 (3), 31001.
Lenormand, E., Sagaut, P., Phuoc, L.T., Comte, P., 2000. Subgrid-scale models for large-Eddy simulations of compressible wall bounded flows. AIAA J. 38, 1340–1350.
Leonard, A., 1974. Energy cascade in large-Eddy simulations of turbulent fluid flows. Adv. Geophys. 18, 237–248.
Leonard, B.P., 1979. A stable and accurate convective modelling procedure based on quadratic upstream interpolation. Comput. Methods Appl. Mech. Eng. 19, 59–98.
Lesieur, M., Metais, O., 1996. New trends in large-Eddy simulations of turbulence. Annu. Rev. Fluid Mech. 28, 45–82.
Lilly, D.K., 1967. The representation of small-scale turbulence in numerical simulation experiments. In: Proceedings of the IBM Scientific Computing Symposium on Environmental Sciences, New York.
Lilly, D.K., 1992. A proposed modification of the Germano subgrid-scale closure method. Phys. Fluids A: Fluid Dyn. 4, 633–635.
Lissaman, P., 1979. Energy effectiveness of arbitrary arrays of wind turbines. J. Energy 3, 323–328.
Liu, S., Meneveau, C., Katz, J., 1994. On the properties of similarity subgrid-scale models as deduced from measurements in a turbulent jet. J. Fluid Mech. 275, 83–119.
Lu, H., Porté-Agel, F., 2010. A modulated gradient model for large-Eddy simulation: application to a neutral atmospheric boundary layer. Phys. Fluids 22, 1–12.
Lu, H., Porté-Agel, F., 2011. Large-eddy simulation of a very large wind farm in a stable atmospheric boundary layer. Phys. Fluids 23, 065101.
Lu, H., Porté-Agel, F., 2013. A modulated gradient model for scalar transport in large-Eddy simulation of the atmospheric boundary layer. Phys. Fluids, 25.
Lund, T.S., 1991. On Dynamic Models for Large Eddy Simulation. Technical Report 177, Annual Research Briefs, Centre for Turbulence Research, Standford University – NASA Ames.
Mann, J., 1994. The spatial structure of neutral atmospheric surface-layer turbulence. J. Fluid Mech. 273, 141–168.
Mann, J., 1998. Wind field simulation. Probab. Eng. Mech. 13, 269–282.
Markfort, C.D., Zhang, W., Porté-Agel, F., 2012. Turbulent flow and scalar transport through and over aligned and staggered wind farms. J. Turbulence 13, 1–36.
Mason, P.J., 1989. Large-Eddy simulation of the convective atmospheric boundary layer. J. Atmosph. Sci. 46, 1492–1516.
Mason, P.J., Brown, A.R., 1999. On subgrid models and filter operations in large Eddy simulations. J. Atmosph. Sci. 56, 2101–2114.
Meneveau, C., Katz, J., 2000. Scale-invariance and turbulence models for large-Eddy simulation. Annu. Rev. Fluid Mech. 32, 1–32.
Meyers, J., Meneveau, C., 2010. Large Eddy simulations of large wind-turbine arrays in the atmospheric boundary layer. In: 48th AIAA Aerospace Sciences Meeting Including the New Horizons Forum and Aerospace Exposition, Orlando, Florida.
Meyers, J., Meneveau, C., 2012. Optimal turbine spacing in fully developed wind farm boundary layers. Wind Energy 15, 305–317.
Meyers, J., Meneveau, C., 2013. Flow visualization using momentum and energy transport tubes and applications to turbulent flow in wind farms. J. Fluid Mech. 715, 335–358.
Michelsen, J.A., 1992. Basis3d – A Platform for Development of Multiblock PDE Solvers. Technical Report AFM 92-06, Department of Fluid Mechanics, Technical University of Denmark.
Michelsen, J.A., 1994. Block Structured Multigrid Solution of 2D and 3D Elliptic PDE's. Technical Report AFM 94-06, Department of Fluid Mechanics, Technical University of Denmark.
Moeng, C.H., 1984. A large Eddy simulation model for the study of planetary boundary-layer turbulence. J. Atmosph. Sci. 41 (13), 2052–2062.
Norris, S., 2000. A Parallel Navier–Stokes Solver for Natural Convection and Free Surface Flow (Ph.D. thesis). School of Aerospace, Mechanical and Mechatronic Engineering, University of Sydney, Australia.

Norris, S., Storey, R., Stol, K., Cater, J., 2012. Modeling gusts moving through wind farms. In: 50th AIAA Aerospace Sciences Meeting Including the New Horizons Forum and Aerospace Exposition, Nashville, Tennessee.
OpenFOAM, The open source CFD toolbox, version 2.2.2, OpenCFD Limited (ESI Group), URL ⟨http://www.openfoam.com⟩, 2014 (Accessed 12 February 2014).
Panofsky, H., Dutton, J., 1984. Atmospheric Turbulence: Models and Methods for Engineering Applications. John Wiley & Sons, New York.
Park, J., Manuel, L., Basu, S., 2012. LES of wind fields and wind turbine load estimation. In: 50th AIAA Aerospace Sciences Meeting Including the New Horizons Forum and Aerospace Exposition. Nashville, Tennessee.
Park, J., Basu, S., Manuel, L., 2013. Large-Eddy simulation of stable boundary layer turbulence and estimation of associated wind turbine loads. Wind Energy. URL http://dx.doi.org/10.1002/we.1580.
Perić, M., Ferziger, J., 2002. Computational Methods for Fluid Dynamics, 3rd ed. Spring-Verlag, Berlin.
Pope, S.B., 2000. Turbulent Flows. Cambridge University Press, Cambridge.
Porté-Agel, F., 2004. A scale-dependent dynamic model for scalar transport in large-Eddy simulations of the atmospheric boundary layer. Boundary-Layer Meteorol. 112, 81–105.
Porté-Agel, F., Meneveau, C., Parlange, M.B., 2000. A scale-dependent dynamic model for large-eddy simulation: application to a neutral atmospheric boundary layer. J. Fluid Mech. 415, 261–284.
Porté-Agel, F., Lu, H., Wu, Y.T., 2010. A large-Eddy simulation framework for wind energy applications. In: Fifth International Symposium on Computational Wind Engineering. Chapel Hill, North Carolina.
Porté-Agel, F., Wu, Y.T., Lu, H., Conzemius, R.J., 2011. Large-eddy simulation of atmospheric boundary layer flow through wind turbines and wind farms. J. Wind Eng. Ind. Aerodyn. 99, 154–168.
Porté-Agel, F., Lu, H., Wu, Y.-T., 2014. Interaction between large wind farms and the atmospheric boundary layer. Proc. IUTAM 10, 307–318.
Réthoré, P.E., 2009. Wind Turbine Wake in Atmospheric Turbulence (Ph.D. thesis). Department of Civil Engineering, Aalborg University, Denmark.
Sagaut, P., 2006. Large Eddy Simulation for Incompressible Flows, 3rd ed. Springer-Verlag, Berlin.
Sanderse, B., 2011. ECNS: Energy-Conserving Navier–Stokes Solver: Verification for Steady Laminar Flows. Technical Report ECN-E-11-042, Energy Research Centre of the Netherlands.
Sanderse, B., 2013a. Energy-conserving Discretization Methods for the Incompressible Navier–Stokes Equations (Ph.D. thesis). Department of Mathematics and Computer Science, Eindhoven University of Technology, Eindhoven.
Sanderse, B., 2013b. Energy-conserving Runge–Kutta methods for the incompressible Navier–Stokes equations. J. Comput. Phys. 233, 100–131.
Sanderse, B., van der Pijl, S., Koren, B., 2011. Review of computational fluid dynamics for wind turbine wake aerodynamics. Wind Energy 14, 799–819.
Schelz, W., Umana, A., Barthelmie, R., Larsen, G., Rados, K., Lange, B., Schepers, G., Hegberg, T., 2001. ENDOW: improvement of wake models within offshore wind farms. Wind Eng. 25, 281–287.
Schepers, J.G., 2012. Engineering Models in Wind Energy Aerodynamics: Development, Implementation and Analysis Using Dedicated Aerodynamic Measurements (Ph.D. thesis). Faculty of Aerospace Engineering, Delft University of Technology, Delft.
Schmitt, F.G., 2007. About Boussinesq's turbulent viscosity hypothesis: historical remarks and a direct evaluation of its validity. Compt. Rendus Mécanique 335, 617–627.
Sforza, P., Sheerin, P., Smorto, M., 1981. Three-dimensional wakes of simulated wind turbines. AIAA J. 19, 1101–1107.
Shen, W.Z., Sørensen, J.N., Mikkelsen, R., 2005. Tip loss correction for actuator/Navier–Stokes computations. J. Solar Energy Eng. 127, 209–213.
Smagorinsky, J., 1963. General circulation experiments with the primitive equations, Part 1: the basic experiment. Mon. Weather Rev. Am. Meteorol. Soc. 91, 99–164.
Smith, D., Taylor, G.J., 1991. Further analysis of turbine wake development and interaction data. In: Proceedings of the 13th BWEA Wind Energy Conference, Swansea, UK.
Snel, H., 1998. Review of the present status of rotor aerodynamics. Wind Energy 1, 46–69.
Snel, H., 2003. Review of aerodynamics for wind turbines. Wind Energy 6, 203–211.
Sørensen, N.N., 1995. General Purpose Flow Solver Applied to Flow Over Hills (Ph.D. thesis). Risø National Laboratory, Roskilde, Denmark.
Sørensen, J.N., 2011. Instability of helical tip vortices in rotor wakes. J. Fluid Mech. 682, 1–4.
Sørensen, J.N., Shen, W.Z., 2002. Numerical modelling of wind turbine wakes. J. Fluid Eng. 124, 393–399.
Stevens, R.J.A.M., Gayme, D.F., Meneveau, C., 2013. Effect of turbine alignment on the average power output of wind-farms. In: International Conference on Aerodynamics of Offshore Wind Energy Systems and Wakes, Lyngby, Denmark.
Stevens, R.J.A.M., Graham, J., Meneveau, C., 2014. A concurrent precursor inflow method for Large Eddy simulations and applications to finite length wind farms. Renew. Energy 68, 46–50.
Stoll, R., Porté-Agel, F., 2006. Dynamic subgrid-scale models for momentum and scalar fluxes in large-Eddy simulations of neutrally stratified atmospheric boundary layers over heterogeneous terrain. Water Resour. Res. 42, W01409.
Stoll, R., Porté-Agel, F., 2008. Large-Eddy simulation of the stable atmospheric boundary layer using dynamic models with different averaging schemes. Boundary-Layer Meteorol. 126, 1–28.
Storey, R.C., Norris, S.E., Stol, K.A., Cater, J.E., 2012. Large Eddy simulation of dynamically controlled wind turbines in an offshore environment. Wind Energy. URL http://dx.doi.org/10.1002/we.1525.
Stull, R.B., 1998. An Introduction to Boundary Layer Meteorology. Kluwer Academic Publishers, Dordrecht, The Netherlands.
Taylor, G.J., 1990. Wake Measurements on the Nibe Wind Turbines in Denmark. Technical Report CEC contract EN3W0039UK, UK National Power.
Tenaud, C., Pellerin, S., Dulieu, A., Ta Phuoc, L., 2005. Large Eddy simulations of a spatially developing incompressible 3D mixing layer using the $v-\omega$ formulation. Comput. Fluids 34, 67–96.
Tennekes, H., Lumley, J.L., 1972. A First Course in Turbulence. MIT Press, Cambridge, MA.
Thomsen, K., Sørensen, P., 1999. Fatigue loads for wind turbines operating in wakes. J. Wind Eng. Ind. Aerodyn. 80, 121–136.
Troldborg, N., 2009. Actuator Line Modeling of Wind Turbine Wakes (Ph.D. thesis). Department of Mechanical Engineering, Technical University of Denmark, Lyngby, Denmark.
Troldborg, N., Sørensen, J.N., Mikkelsen, R., Srensen, N.N., 2013. A simple atmospheric boundary layer model applied to large Eddy simulations of wind turbine wakes. Wind Energy. URL http://dx.doi.org/10.1002/we.1608.
van der Pijl, S.P., 2007. Numerical Modelling of Wind Farm Aerodynamics. Technical Report ECN Internal, Energy Research Centre of the Netherlands.
Vermeer, L.J., Sørensen, J.N., Crespo, A., 2003. Wind turbine wake aerodynamics. Prog. Aerosp. Sci. 39, 467–510.
Verstappen, R.W.C.P., Veldman, A.E.P., 2003. Symmetry-preserving discretization of turbulent flow. J. Comput. Phys. 187, 343–368.
Wan, F., Porté-Agel, F., 2011. Large-Eddy simulation of stably-stratified flow over a steep hill. Boundary-Layer Meteorol. 138, 367–384.
Wan, F., Porté-Agel, F., Stoll, R., 2007. Evaluation of dynamic subgrid-scale models in large-Eddy simulations of neutral turbulent flow over a two-dimensional sinusoidal hill. Atmosph. Environ. 41, 2719–2728.
Wesseling, P., 2001. Principles of Computational Fluid Dynamics, 1st ed. Springer-Verlag, Berlin.
Wilcox, D.C., 2006. Turbulence Modeling in CFD, 3rd ed. DCW Industries, California, USA.
Wu, Y.T., Porté-Agel, F., 2011. Large-eddy simulation of wind-turbine wakes: evaluation of turbine parametrisations. Boundary-Layer Meteorol. 138, 345–366.
Wu, Y.T., Porté-Agel, F., 2012. Atmospheric turbulence effects on wind-turbine wakes: an LES study. Energies 5, 5340–5362.
Wu, Y.T., Porté-Agel, F., 2013. Simulation of turbulent flow inside and above wind farms: model validation and layout effects. Boundary-Layer Meteorol. 146, 181–205.
Zang, Y., Street, R.L., Koseff, J.R., 1993. A dynamic mixed subgrid-scale model and its application to turbulent recirculating flows. Phys. Fluids A: Fluid Dyn. 5, 3186–3196.
Zhang, W., Markfort, C.D., Porté-Agel, F., 2013. Wind-turbine wakes in a convective boundary layer: a wind-tunnel study. Boundary-Layer Meteorol. 146, 161–179.